# AN EXPERIMENT TO MEASURE LASER BEAM WANDER AND BEAM SPREAD IN THE MARINE BOUNDARY LAYER NEAR SHORE

David Albert Beall

# NAVAL POSTGRADUATE SCHOOL
## Monterey, California

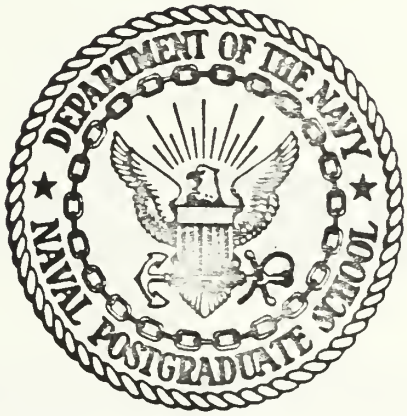


# THESIS

AN EXPERIMENT TO MEASURE LASER BEAM WANDER
AND BEAM SPREAD IN THE MARINE BOUNDARY LAYER
NEAR SHORE

by

David Albert Beall

Thesis Advisor: E. C. Crittenden, Jr.

December 1973

*Approved for public release; distribution unlimited.*

# An Experiment to Measure Laser Beam Wander and Beam Spread In The Marine Boundary Layer Near Shore

by

David Albert Beall
Lieutenant Commander, United States Navy
B.A., University of Washington, 1961

Submitted in partial fulfillment of the
requirements for the degree of

MASTER OF SCIENCE IN PHYSICS

## ABSTRACT

A system to measure laser beam wander and beam spread in the atmosphere over the ocean has been designed, constructed, and tested. The apparatus employed a high resolution scanning telescope with a potential for use in a broad range of visual and infra-red wavelengths, and with the ability to measure beam wander and beam spread variations on the order of a few microradians in angle of incidence. Three successful trials with a propagation path over the southern end of Monterey Bay were conducted. Data was processed using analog and digital computers. RMS values of beam wander from 4.6 to 30.2 microradians were observed.

TABLE OF CONTENTS

TABLE OF CONTENTS Cont

## LIST OF TABLES

## LIST OF DRAWINGS

## ACKNOWLEDGEMENT

The author wishes to express his appreciation to all the members of the atmospheric propagation group of the Physics Department. A special note of gratitude is extended to Professor Eugene C. Crittenden, Jr., whose contributions to the design, construction and operation of apparatus far exceeded any responsibilities as a thesis advisor, and to LCDR Arthur F. Schroeder, whose work on transmitter optics and general cooperation significantly enhanced the work reported here. In addition, it is gratefully noted that the experiments conducted would not have been possible without the cooperation of the management of the Holiday Inn Motel, Seaside, California, and Hopkins Marine Station, Monterey, California, which provided facilities for the experiments, and the Weapons and Equipment Division, U.S. Army, Fort Ord, California, which has provided all communications equipment used by the group for the past year.

# I. PROBLEM DESCRIPTION

With the increasing knowledge and application of lasers in our society it has become important to understand more fully the ways in which a laser beam interacts with the medium through which it passes. Of particular importance are the effects of ordinary air, with its variations in density, temperature, humidity, and particulate content. There are two broad classes into which these effects may be categorized. The first class is only seen when high power beams are used, and are brought about when a significant amount of laser energy is transfered to the medium, causing meteorological phenomena over and above those that would be present normally. These phenomena in turn have an effect on the beam. Thermal blooming and up-wind drift are examples of such non-linear disturbances. The second class are those effects which are due only to naturally occurring atmospheric fluctuations. Such effects may be observed in both low and high power beams. They include absorption, scattering, Modulation Transfer Function (MTF) variation, scintillation, beam wander, and beam spread. This thesis deals with the latter two phenomena as they occur in the atmosphere near the ocean surface. In particular, the development of an experiment to measure beam wander and beam spread in the atmosphere immediately above the sea surface will be described, together with some preliminary results of a small number of trials of such an experiment.

It should be emphasized that the objectives of the work reported herein were somewhat limited from the outset. Due to the fact that the primary research ship, the R.V. ACANIA, was required for numerous other Naval Postgraduate School projects, that none of the apparatus was previously designed or assembled, and that the entire question of beam wander and beam

spread over the ocean was relatively unexplored, it was envisioned that the task of developing a fully comprehensive experiment, with the capability of operating over the open ocean and more than one optical wavelength, would require the efforts of two or more successive thesis students. Thus, this is just the first report on what is expected to be an ongoing project.

## A. MATHEMATICAL DESCRIPTION OF BEAM WANDER AND BEAM SPREAD

Since the index of refraction of a medium depends upon its density, a beam passing through a medium with variations in density may be expected to follow a path which is not straight. If the diameter of the beam is not much less than the transverse distance in which significant variations occur, then the bending of the beam will be fairly complicated, since different portions of the beam will pass through regions of different refractive index. Thus, the beam will change shape, change direction, and exhibit regions within its cross-section where interference causes greater or less intensity than would be expected in a medium with constant density. These effects are known respectively as beam spread, beam wander and scintillation. Obviously, these same effects will also occur in any beam regardless of diameter if significant variation in density along the path of propagation is present. In the atmosphere normal meteorological conditions commonly cause both longitudinal and transverse density variations over a range of scales sufficient to induce such effects in beams of all sizes. In fact turbulence scales near the earth's surface may be expected to range from the order of one millimeter to a few meters [Ref. 1]. The term, turbulence scale, is somewhat loosely defined. It may be roughly visualized as the diameter of a turbule, or region where the air rotates about a common point. Over a path of, say, 1km, then one might expect at least $10^3$ to $10^6$ such turbules.

Clearly a statistical model is the only formulation which could be expected to describe the effects of turbulence on a laser beam. The only successful models existent require the assumption of randomness of transverse refractive index fluctuation. The preeminent basis for such models was introduced by Tatarski [Ref. 2]. First, $C_n$, the refractive index structure constant, is defined.

$$C_n(\bar{r}) = [D_n(\bar{r})]^{1/2} r^{-1/3}, \quad l_0 < r < L_0, \tag{1}$$

where

$$D_n(\bar{r}) = \langle [n(\bar{R}) - n(\bar{R}+\bar{r})]^2 \rangle_{av}. \tag{2}$$

Here, $\bar{r}$ = a vector between two points in the transmitter aperature,

$\bar{R}$ = a vector to any point within the common area of two circles with centers at the endpoints of $\bar{r}$,

$n$ = the index of refraction at a point,

$l_0$ = the smallest turbulence scale present,

$L_0$ = the largest turbulence scale present,

av = indicates an ensemble average over all realizations of the atmosphere for fixed meteorological conditions.

Fortunately $C_n$ can be measured, so that analytical solution of (1) and (2) is not required. This can be done either through measurement of scintillation or micrometeorological observations. Recent measurements of $C_n$ by Haagensen [Ref. 3] demonstrate that meteorological and optical measurement of $C_n$ over the ocean surface are well correlated.

Tatarski showed that a power spectrum based on refractive index fluctuations is proportional to the velocity spectrum of the turbulence [Ref. 2]. From this fact, plus the assumption of isotropy which allows the conversion of (1) and (2) to scalar equations, Strohbehn developed an expression for a refractive index power spectrum, $\phi_n(K)$, [Ref. 1]:

$$\phi_n(K) = 0.033C_n^2 \exp(-K^2/K_m^2) K_0^{-11/3} (1+K^2/K_0^2)^{-11/6} \quad (3)$$

where,

$K$ = spatial wave number,

$K_m = 5.92/l_0$,

$K_0 = 2\pi/L_0$.

From $\phi_n(K)$, a wave structure function, $D(r,z)$, can be developed [Refs. 1, 2, 4].

$$D(r,z) = 4\pi k_0^2 z \int_0^1 dy \int dK \phi_n(K)\{1-\exp[iKr(1-y)]\},$$

where,

$z$ = distance along the beam from the transmitter,

$k_0$ = optical frequency wave number.

$D(r,z)$ can be inserted in the form of a weight function into the Fresnel-Kirchhoff integral to give a time averaged irradiance in the receiver plane,

$$I(\bar{w}) = (k_0^2/2\pi z) \int d\bar{r} F(\bar{r},z) \exp[-1/2D(r,z)] \exp[-iK\bar{w}\cdot\bar{r}/z] \quad (5)$$

where,

$w$ = position in the receiver plane,

$F(\bar{r},z)$ = the aperature function projected through the distance z.

That is,

$$F(\bar{r},z) = \int dR U(R+1/2r) U^*(R-1/2r) \exp(ik_0\bar{R}\cdot\bar{r}/z) \quad (6)$$

where U is the amplitude of the radiation in the aperature [Ref. 4].

As pointed out in Ref. 4, equation (5) is not susceptible in general to analytic solution for beam wander and spread. However, several approximations have been made [Refs. 4, 5, 6, 7, 8, 9]. These generally give an expression for beam wander or beam spread in terms of $C_n$, z, and either $K_0$ or $l_0$. Dowling and Livingston have tabulated many of these expressions in common units and dimensions in Ref. 4. For example, their own expression,

based partly on work by Fried, gives beam wander, defined as the mean square motion of the energy centroid as

$$\phi^2 = 32\pi^2 zf/3L_1, \tag{7}$$

where,

$$L_1 = 1/[1/2X0.0330C_n^2(1_0/5.92)^{1/2}], \tag{8}$$

f = a complicated function of transmitter aperature and turbulence developed by Fried, which is independent of z, $k_0$, and $C_n$[Refs. 4, 10].

Dowling and Livingston also show that assuming a gaussian beam,

$$\theta'^2 = \theta^2+\phi^2, \tag{9}$$

where,

$\theta$ = short term average beam width expressed as the angle in radians from the transmitter subtended by the $1/e^2$ power distribution width in the focal plane (waist) of the beam,

$\theta'$ = long term average beam width expressed in the same terms [Ref. 4].

In figure 1 of Ref. 8, Chiba gives a partly qualitative graph, which would seem general enough to cover all the approximations of the Tatarski model in representing the increase of beam wander with turbulence.

## B. BROAD DESIGN CRITERIA FOR THE APPARATUS

### 1. Uniqueness of the Experiment

At the outset of the investigation no other experiment to measure beam wander or spread over the open ocean was known to have been conducted or to be in progress. This placed certain constraints on design. In particular, the relatively high probability that any particular complete experiment would not be successful indicated a fairly cautious approach. Each component would be built, tested indoors, and possibly rebuilt and retested before inclusion in the experimental system. The entire system was tested in a 400 foot hallway before the first over-water trial.

2. Portability

A fairly compact portable apparatus was required for three reasons. First, as mentioned above, it was deemed important to test the apparatus indoors preliminary to over-water experiments. Second, although to date the experiment has been conducted successfully across bays, that is with the apparatus on one shore and the transmitting laser on the other, it is desirable that it ultimately be conducted between two ships if possible or at least from ship to shore. This is due to uncertainties as to the effect some shoreline profiles may have on atmosphere flow patterns. Third, it was not known whether the relative unchangeability of weather conditions in the vicinity of Monterey would provide a sufficient base for correlations with beam wander and spread. Thus, it might have been necessary to conduct the experiment in other locales.

3. Precision

Overland measurements of beam wander by Dowling and Livingston [Ref. 4], and by Chiba [Ref. 8] indicated that variations in beam direction on the order of 100 microradians for path lengths in the kilometer range might be expected. This indicated the requirement for high quality optics, precision scanning, and a means for compensating for motion involved in tracking a moving target, i.e., the shipboard laser. In fact, RMS beam wander measurements on the order of 10 microradians have been generally observed on cross bay experiments.

4. Scan Repetition Rate

Concerning the possible characteristic frequencies which might be associated with beam wander, data from Ref. 4, as well as subjective observations of laser beam behavior on previous experiments, such as the scintillation work by Haagensen [Ref. 3], indicated that frequencies in the 1 to 10 Hz regime might be expected. Thus at a minimum, the apparatus

should be capable of scanning the beam or an image of the beam on the order of 100 times a second.

5. Wavelength Capability

The experiment as designed and conducted to date has utilized a source of 6328 Angstrom He-Ne laser radiation. However, it is desirable that in the future the apparatus be used in the infra-red range out to 10.6 microns. Thus it was designed as much as possible with front surface reflective optics to provide a broad band capability.

## II. DEVELOPMENT OF THE APPARATUS

### A. BASIC CONCEPT

As noted above, beam wander and spread measurements over land were made by Dowling and Livingston in 1972 [Ref. 4]. Their apparatus was straightforward, consisting of two laser beams, one at 6328 Angstroms and one at 10.6 microns, transmitted by a Newtonian telescope to a 91.5 cm diameter spherical mirror at the receiver site. The receiver was located at the focal plane of the beam. The radiation reflected from the 91.5 cm mirror was brought to a small diameter on a galvanometer mirror, which in turn sent images to two slits, one for each wavelength, behind which detectors were located. In effect an image of a small portion of the 91.5 cm mirror was placed at each slit. With the galvanometer mirror movement driven by a triangle waveform current, an entire diameter of the mirror was scanned at a repetition rate of 75 Hz. One of the two systems reported by Chiba [Ref. 8] employed a position sensitive detector. The other was largely similar to the system used by Dowling and Livingston.

The relative lack of portability, questionable ability for tracking a moving target, and cost of a high quality concave mirror of the size required obviated the above approach for an early over-water experiment. Rather it was decided to use the principle of reversibility in the Naval Postgraduate School apparatus. The telescope would be placed at the receiver, rather than the transmitter, and the image to be scanned would be the image of the source, rather than that of the beam focal plane. Assuming that the turbulence is symmetric in the propagation direction about the mid-point of the propagation path, the principle of reversibility yields that the motion of the image of a stationary laser cavity due to atmospheric

refractions is the same as if the image were stationary and the object in motion. The diffraction limited image gathered from defocused light of the laser is equivalent to the intensity distribution of the focused laser radiation when viewed at its waist, i.e., its diffraction limited focal plane.

Thus the basic concept was to use a divergent laser beam as a source, and record the motion and shape of the image of the laser crossover point (Figure 1) formed by the telescope.

## B. EARLY CONFIGURATION OF APPARATUS

### 1. Telescope

The first telescope built used a 9.2 cm diameter, 92.4 cm focal length parabolic mirror previously used by Hildebrand [Ref. 11] in atmospheric MTF research. This was combined with a 3.8 cm diameter, 24.5 cm focal length convex spherical mirror and a flat 90 degree turning mirror in a Cassegranian telescope. The arrangement is shown in Figure 2. This telescope had an equivalent focal length of approximately 6.6 meters.

### 2. Scanner

The first scanning device built employed an eight sided prism which was rotated at about 60 Hz. A magnetic field was provided perpendicular to the axis of rotation. The prism mounting had eight narrow grooves parallel to the rotation axis, one beneath each corner of the prism. A tape recorder magnetic playback head was located adjacent to the prism mounting. As the grooves on the mounting passed the playback head, they caused perturbations in the magnetic field, which activated a signal in the playback head. This signal was used to trigger an oscilliscope. The prism was positioned in the output optical path of the telescope. The rotation of the prism caused the image formed by the telescope and prism to be scanned across a slit, behind

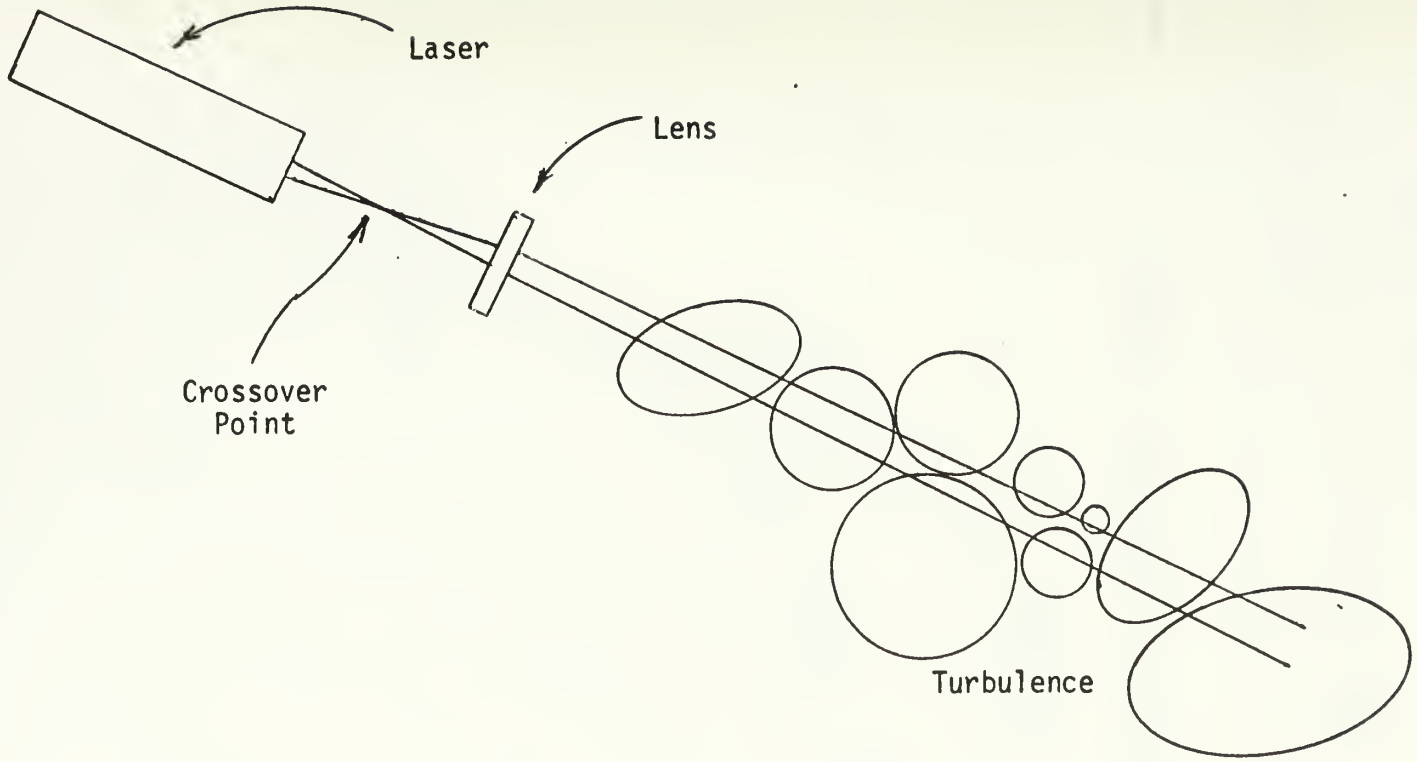


FIGURE 1. Transmitter Optics and Propagation Path

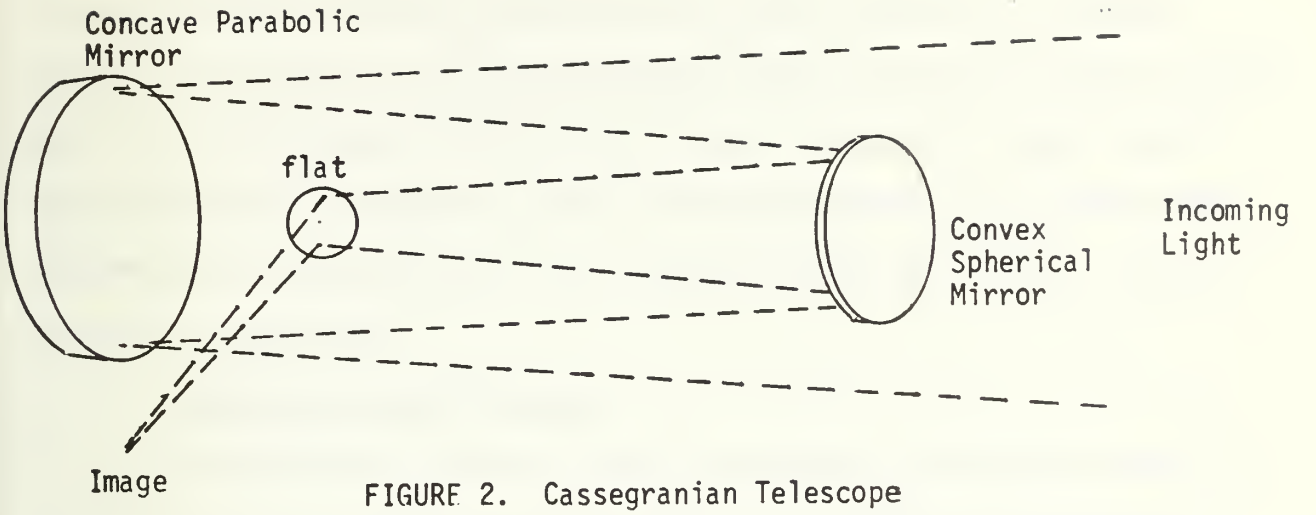


FIGURE 2. Cassegranian Telescope

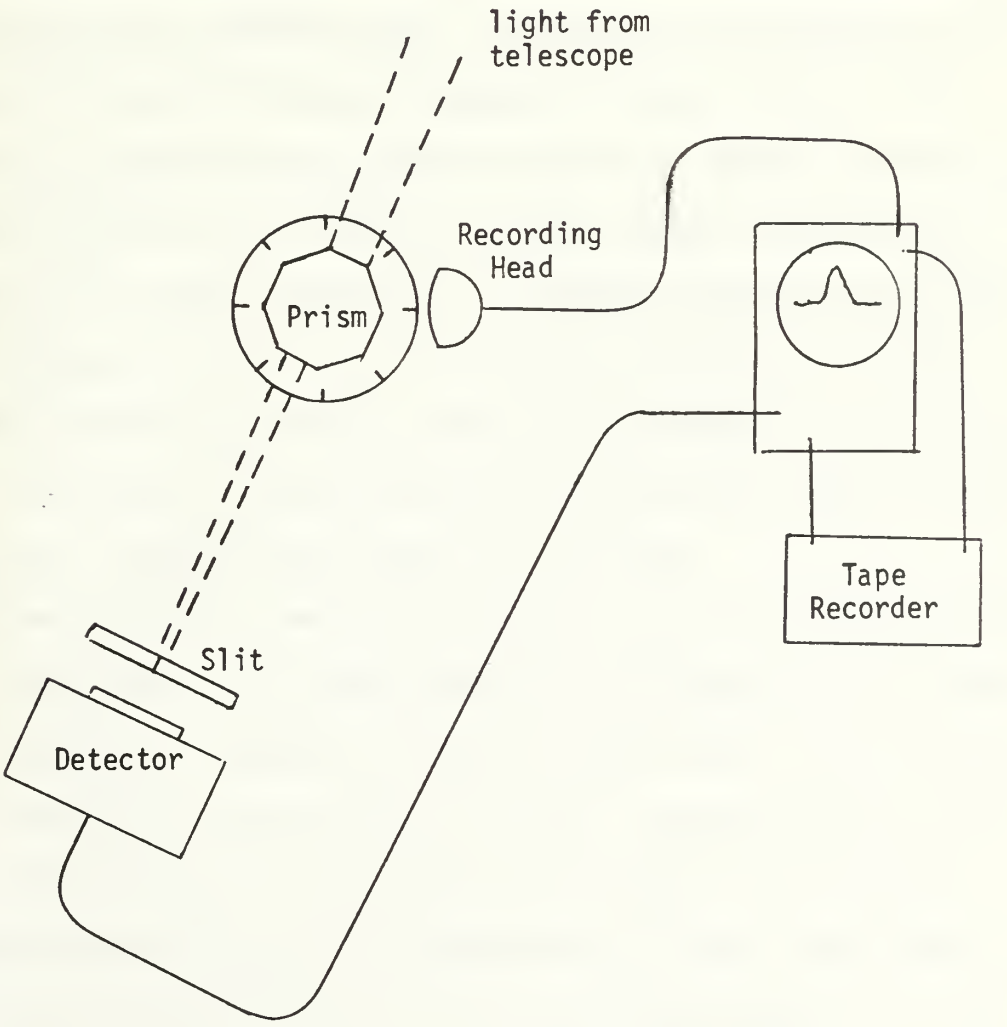


FIGURE 3. Eight Sided Prism Scanner

which a detector was mounted. The signal from the detector was fed to the vertical input of the oscilloscope and to a tape recorder for storage. Thus, if the grooves in the prism mounting could be located precisely enough, and the rotation speed could be kept constant, consecutive images scanned past the slit would appear as optical intensity curves on the oscilloscope referred to a fixed position in the image plane and be recorded. Figure 3 shows this arrangement.

3. Advantages and Difficulties

The practical problem of cutting the grooves in the prism mount and positioning the prism with sufficient accuracy to stabilize the image on the oscilloscope proved insurmountable. Therefore it was necessary to use only one out of every eight images transmitted, in order that the image displayed have a constant phase relationship with the magnetic groove trigger signal. Thus only about eight usable images per second were available, obviously too few for good resolution of a phenomena expected to have characteristic frequencies in the 1 to 10 Hz range. In addition, the prism obviated the capability to operate in the visual and infra-red regions simultaneously. No material with good transmission and suitable mechanical properties in such a broad band was known to be available.

The secondary mirror was manufactured by silvering a lens to provide near 100% reflectance. This mirror produced some astigmatism in the image in certain directions. Although good quality convex mirrors are available, the other considerations mentioned above caused a reconfiguration of the apparatus, and the Cassegranian telescope was discarded in the process.

Despite these faults, this configuration had many strong features. As foreseen by Hildebrand in Ref. 4, it eliminated the nuisance of having successive images displayed with reversed positive direction of the abscissa, which occurs in galvanometer type scanners. The Cassegranian telescope

allowed a relatively high magnification in a reasonably short telescope, i.e., the ratio of the focal length to the telescope length was about four. Despite the problem of astigmatism, the magnification achieved produced excellent structure resolution in the image. Figure 4 shows some of the images produced by this system. The object was the optical crossover point of a 6328 Angstrom, 0.1 mW TM 00 laser with divergent optics which provided a virtual object distance of 104 m. The laser was located about four fifths of this distance from the telescope in a hallway with numerous ventilators in the overhead. Scintillation and beam wander are clearly visible. Exposure time was greater than the scan time, so that more than one image is seen in each photograph. The less bright lines are persistent traces of images displayed before the camera shutter was opened.

C. PRESENT CONFIGURATION OF APPARATUS

Despite the advantages of the system described above, its disadvantages were too great to be overcome. Thus, a new system has been developed, which employs galvanometer mirror scanning and a Newtonian telescope. The primary mirror is a 25.4 cm diameter 204.5 cm focal length spherical mirror. Its reflected light is intercepted just short of the focal plane by a flat mirror oriented 45 degrees from the telescope axis, and transmitted through a filter and diverging lens at the top of the telescope. Here it is turned by another 45 degree mirror and brought to a focus in front of the scanning mirror. It is reflected from the concave scanning mirror, passes back between the upper folding mirror and the diverging lens, and is brought to a focus on a vertical slit. A detector is mounted directly behind the slit. The positions of both folding mirrors, the diverging lens, the galvanometer mirror, and the slit/detector assembly are adjustable so that an image may be formed at the plane of the slit for object distances from 100 meters to

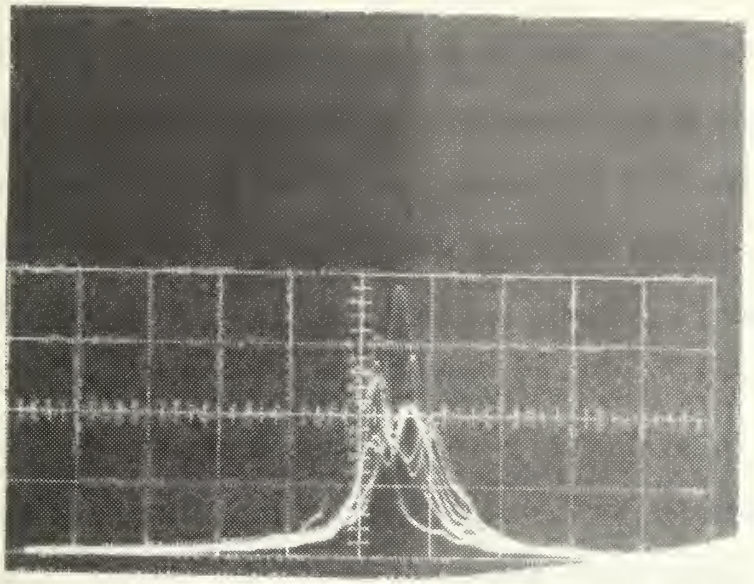

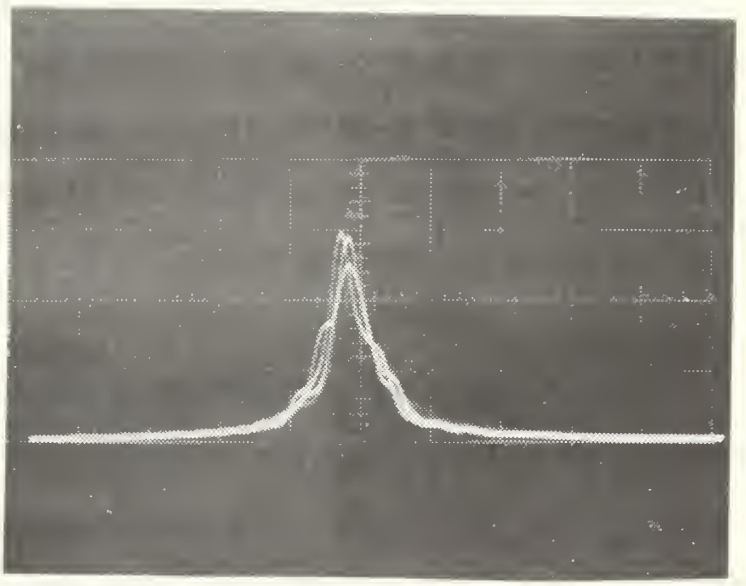

FIGURE 4. Images Obtained With Cassegranian Telescope
And 2 Sided Prism Scanner Intensity vs.
Horizontal Position In The Image Plane.

infinity. In addition, the mounting for the upper folding mirror, scanner, and slit/detector assembly can be rotated through a complete circle in the horizontal plane. This allows the beam to be scanned through a linear path at any angle in its transverse plane without rotating the whole telescope. Figures 5, 6, and 7 show the telescope and scanner assembly.

To operate the galvanometer as a scanner, it was necessary to replace its suspension with a stiffer wire, since the original gold foil suspension was not expected to be rugged enough to survive transportation to the field.

The sinusoidal drive current causes the galvanometer movement to act as a forced harmonic oscillator, with the input current as the forcing function. Thus the angular deflection of the mirror is sinusoidal in time, with the same frequency as the drive current. The phase angle between the driving current and the mirror deflection is constant once steady state has been achieved [Ref. 12]. Tests of the scan mirror showed that the center of the angular deflection remained constant to within 0.004 of the amplitude of the deflection. For the instrument settings used in subsequent over-water experiments, this corresponds to an accuracy of about 2.8 microradians in beam wander.

To provide fine steering of the galvanometer, a variable D.C. bias voltage is applied to the driving current. This has the effect of shifting the center of the scan. It was envisioned that this bias voltage could be removed during data reduction. However, up to the present, this voltage has been used only to set the scan center prior to starting data collection, and variation has not been required during collection itself.

The detector is an E.G.&G. Incorporated SGD-444 silicon photodiode. The slit opening is adjustable and has been used at various settings during the experiments conducted. The largest slit opening used has been 0.066 mm, and the preponderance of the data has been collected with a slit opening of

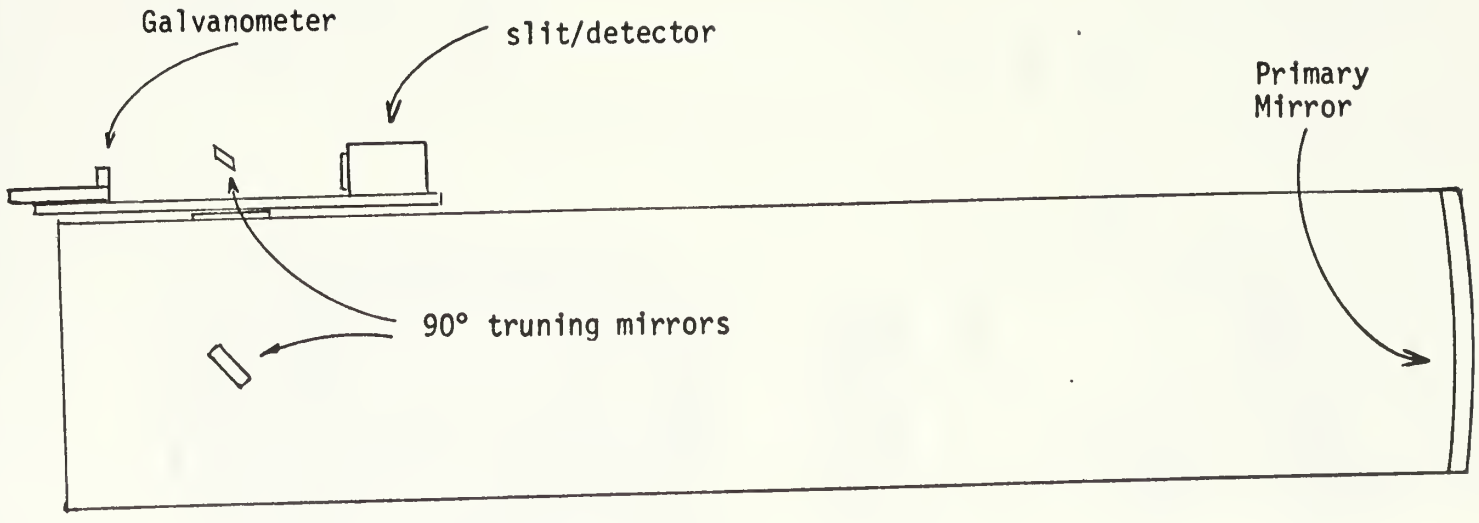


FIGURE 5. Newtonian Telescope and Scan Assembly

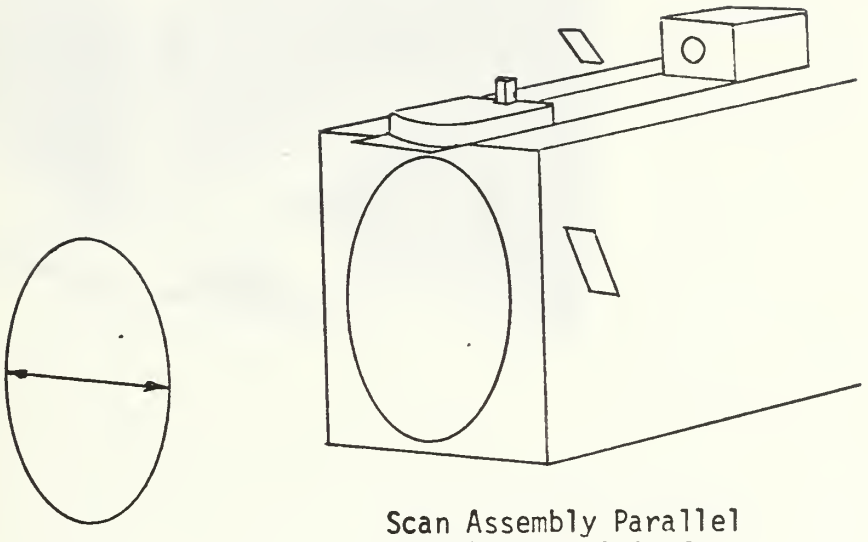

Scan Assembly Parallel
to Telescope Axis for
Horizontal Scan

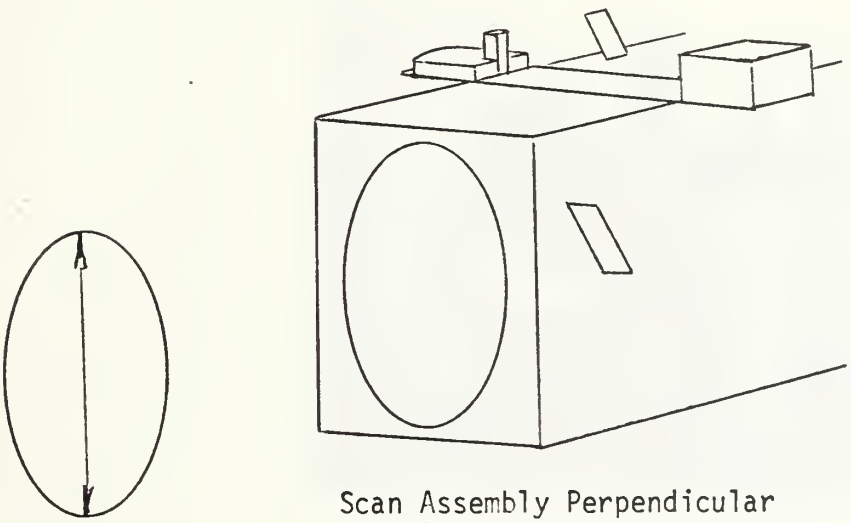

Scan Assembly Perpendicular
to Telescope Axis for
Vertical Scan

FIGURE 6. Scan Assembly Showing Effect of
Rotation of Sampling Direction

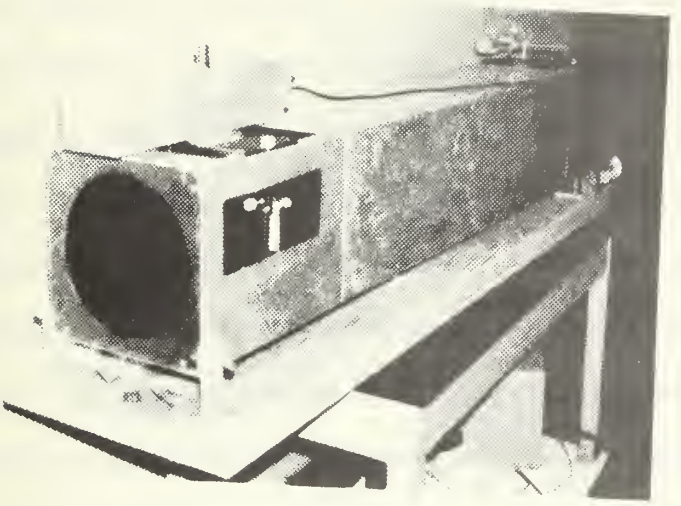

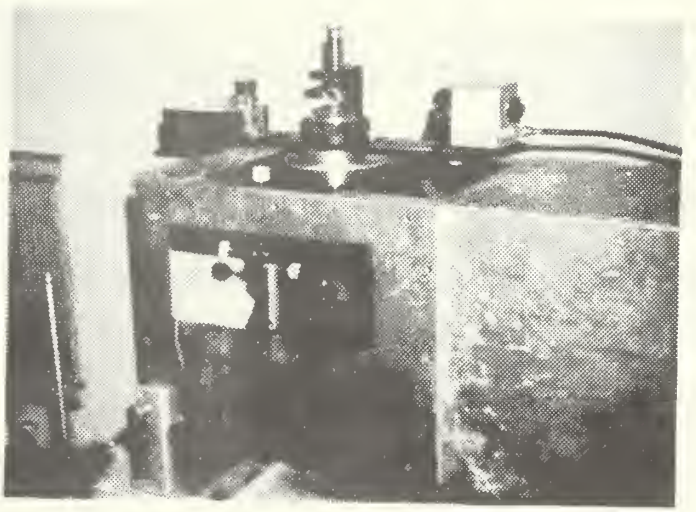

FIGURE 7. Photograph of Telescope and Scanner

0.045 mm. Slit calibration was obtained with a traveling microscope. The length of the slit is 1.5 cm.

Since there is no provision for eliminating motion of the image along the length of the slit due to beam wander and spread in the direction perpendicular to that being scanned, the question of the uniformity of the response of the detector is important. This has been measured with the result that a constant intensity beam trained along the length of the slit produced a maximum deviation of 2.5 percent in the detector response. This figure may be somewhat low, however, since the beam used was about twice the diameter of the images commonly seen in the field experiments, thus allowing some averaging effects.

The entire scanning/detecting assembly is provided with a cover to reduce side and back light. The cover is not completely light tight, however this is only a matter of convenience, since low frequency intensity levels are removed during data processing.

The detector signal is displayed on an oscilloscope, which also amplifies it and outputs it to a bias control circuit. It is then passed through a 10:1 amplifier to a Hewlett-Packard 3960E F.M. four channel instrument tape recorder. The recorder is operated at 15 inches per second, providing 0 to 5000 Hz frequency response. Thus, it is possible to record 10,000 intensity levels per second. The recorder responds to input voltages in the range -10 to 10 volts. Since the image intensity is always a positive signal, the bias control circuit allows use of the full voltage range of the recorder. This is done by adjusting the bias so that the D.C. level of the input signal is at the minimum (-100% on the recorder level indicator) of the voltage response range. This procedure effectively increases the signal to noise ratio of the recorded signal.

The scan drive signal is also recorded, and at the same time used to trigger the oscilloscope. Figure 8 shows a schematic diagram of the entire system.

Calibration of the system is accomplished using a coarse diffraction grating. To obtain a calibration for a particular set of adjustments on the telescope, the grid is placed in the incoming beam directly in front of the telescope. The grid bar center-to-center separation is 8.95 mm. Thus the distance between the diffraction peaks on the oscilloscope, when using 6328 Angstrom light, corresponds to 70.7 microradians angular deflection of rays entering the telescope. If the X axis of the oscilloscope is driven by the scan drive signal, then the diffraction pattern appears on a linear horizontal scale, and may be used as a calibration. Figure 9 shows the diffraction grid and a typical diffraction pattern it produced.

All of the trials of the experiment discussed below employed the configuration of apparatus just described.

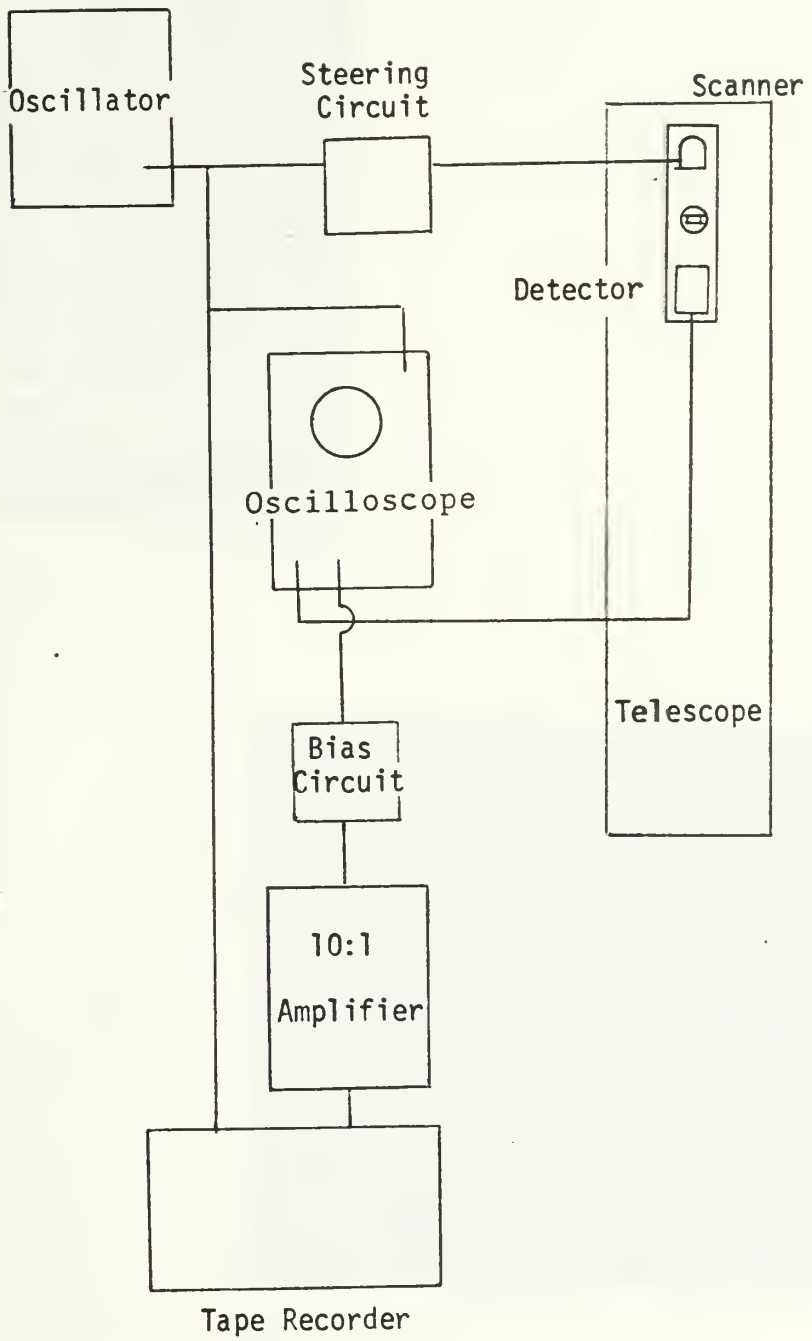


FIGURE 8. Schematic of System

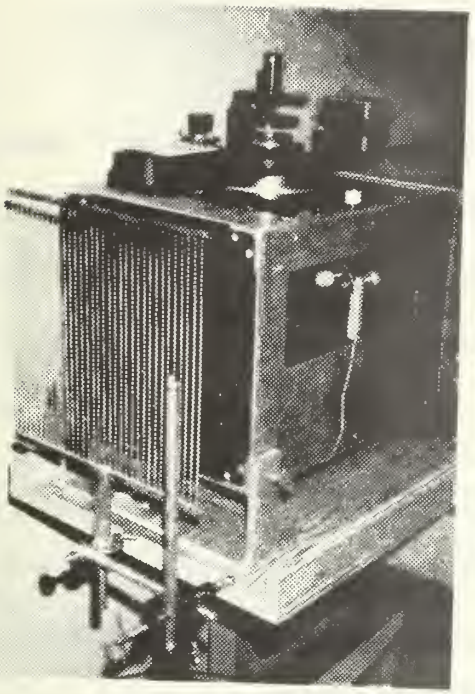

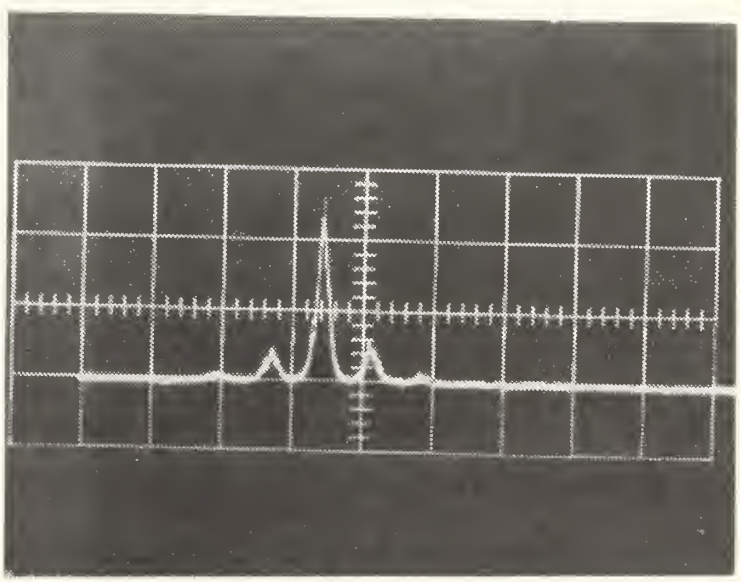

FIGURE 9. Calibration Grid and Diffraction Pattern

## III. EXPERIMENTS

To date, five over-water experiments have been attempted. Only three of these produced successful results. The other two, San Micholas Island, September 1973 and Monterey Bay, November 1973, are discussed briefly, because it is felt that the difficulties encountered can be avoided if known beforehand.

### A. SAN NICHOLAS ISLAND, SEPTEMBER 1973

This experiment was originally scheduled as only a scintillation experiment, with the objectives of testing various details of scintillation theory [Ref. 13] and initially testing a gyro stabilized ship mounted laser. The beam wander and spread experiment was added when it became apparent that the apparatus would be ready in time. Two transmitters were available, one the ship mounted laser aboard the R. V. ACANIA, and the other located ashore across Laser Bay from the receiver site, located on the northwest tip of San Nicholas Island in the Santa Barbara Channel. Equipment was transported to the island by air, and was set up at the site in tents.

Despite all efforts to protect the equipment, a northwest wind of up to 30 knots continually blew sand and salt spray into the tents, making it necessary to keep the apparatus wrapped in plastic and non-functional most of the time. At times, visibility was reduced to a few hundred meters by the amount of sand in the air. In addition, the size of the tents required the front end of the telescope to protrude from the tent door. During attempts to take data the wind caused so much vibration of the telescope that stabilizing the scan was impossible. These conditions, combined with crew fatigue and unforeseen logistic problems, rendered the situation untenable,

and the experiment was cancelled. Lessons learned from this trial were as follows.

The apparatus should be enclosed in a solid structure. For future trips to San Nicholas Island a van should be used.

The shore based crew should arrive and set up well in advance of the ship's arrival. At least two days advance time to set up and test equipment and become acclimatized to the harsh weather conditions on the island should be planned.

Any feasible measure to provide personnel support should be taken. The equipment van should be provided with cooking and sleeping facilities, since the nearest messing and berthing facilities are a 45 minute drive from the receiver site. The only transportation is an open army weapons carrier, and much of the trip to the air terminal/messing/berthing area is over dirt roads that are in extremely poor repair. This fact should be kept in mind when preparing equipment for transportation.

There is no pier on the northern part of the island, and beaching a whale boat is hazardous, since the bay is only slightly protected. Two personnel exchanges between the ship and shore were accomplished, but they required wading out chest deep to the ship's boat. A zodiac boat would probably be capable of beaching.

B. MONTEREY BAY, NOVEMBER 1973

Throughout the development of the beam wander and spread receiver apparatus, a parallel project to manufacture a gyro stabilized laser transmitter for shipboard use was being carried out under Professor Eugene C. Crittenden, Jr. One of the intermediate tests of the gyro system was conducted in November 1973 with the beam wander and spread apparatus as one of the receivers used. A manual tracking system was attached to the telescope. The stabilized transmitter was located aboard the R. V. ACANIA at a distance

from the receiver site of about 1.0 km. Although the stabilization system operated properly, vertical motion of the source due to swells, two to four feet, as well as lateral ship motions were too great to keep the image in the field of view of the telescope.

Based on this attempt, it appears that fully automatic tracking by the receiver will be required for future ship to shore experiments.

C. MONTEREY BAY, 9, 18, AND 22 OCTOBER 1973

These three successful trials were conducted with the transmitter located at the Holiday Inn Motel, in the northern outskirts of Monterey, and the receiver at Stanford University's Hopkins Marine Station, Monterey. The range is shown in Figure 10. The source was a 6328 Angstrom TM 00 laser with 3 mW output. The propagation path was horizontal and was 4.1 km in length. Transmitter and receiver were located 15 feet above the mean high water mark.

On the 9th and 22nd, no meteorological data over the propagation path was available. On the 18th, meteorological $C_n$ measurements were taken aboard the R. V. ACANIA stationed near the mid-point of the propagation path. However, processing of that data has not been completed. Optical $C_n$ measurements were taken for all three days, and have been processed [Ref. 13].

On the 9th and 18th, the prevailing wind was from the west at about 10 knots. Cloud cover varied from 0 to 100 percent. On the 22nd, data was taken after a morning shower. The atmosphere was exceptionally clear. The prevailing wind was from the south at approximately 20 knots, and the sky was clear throughout the trial.

Data was taken quasi-continuously on the 9th and 18th. On the 22nd, data was taken in 50 second periods at 10 minute intervals. The experiments were conducted from 1754 to 2314 9 October, from 1855 to 2154 18 October, and from 1555 to 1754 22 October.


FIGURE 10. Chart of Monterey Bay Test Range

A scan frequency of 120 images per second was used on all three days. As mentioned above, slit openings varied from 0.045 mm to 0.066 mm, with most of the data taken with the former value.

## IV. DATA REDUCTION

The data is processed in five major steps, which are described below.

### A. ANALOG TO DIGITAL CONVERSION

The tape recorded optical intensity and scan drive signals are converted to digital information in the Naval Postgraduate School Electrical Engineering Department Computer Laboratory, using a COMCOR 5000 analog computer and a Scientific Data Systems SDS 9300 computer. When digitized the data are stored as four byte integers in octal representation on seven track magnetic tapes. Operating procedures for the converter and computer may be found in Refs. 14 and 15.

Several programs for A/D conversion are available, and any facility which uses the SDS 9300 will no doubt have such programs available. They are written in XDS FORTRAN, a variant FORTRAN language, and make extensive use of assembler language subroutines. For these reasons, they are not included in this thesis. However, for convenience of Naval Postgraduate School users definitions of variables which must be input by the operator are given below.

NCHAN is the number of channels to be recorded. For this experiment NCHAN is two, however, the A/D system is capable of handling up to eight channels.

NREC is an upper bound on the number of records that will be written on the tape. A record is a block of data recorded on the tape separated from the previous and subsequent record by a space. Division of the data stream into records allows reading and writing on tape to proceed quickly.

NSAMP is the number of samples of each channel per record. NSAMP equal 512 has been used with good results.

ITAPE is the magnetic tape unit number which is set on the magnetic tape console when mounting the tape.

NF is the number of files on the tape to be skipped before commencing recording. A file is a complete set of converted data, i.e., all the data from the interval over which beam wander and spread are to be computed. An end of file (EOF) mark is written on the tape at the conclusion of each file. The EOF mark cannot be passed by a computer when reading the tape, and will trigger the END option of a FORTRAN read statement.

The maximum sample rate at which the system can operate is dependent on the number of channels being digitized. For two channels a sample rate of 3333 samples per second on each channel is possible. However, better results in subsequent processing have been obtained if a sample rate of 2500 is used. Digitizing is done with the original recording played back at 1/4 speed, i.e., 3 3/4 inches per second. Thus, each channel is sampled at 10,000 per second real-time, that is the time reference frame in which the data is collected. This corresponds to the frequency response of the tape recorder. This is believed to be the reason why better results are obtained at the lower sampling rate. This sample rate allows about five files of 15 seconds real-time to be recorded on the 2400 foot seven track computer tape.

B. OCTAL TO HEXADECIMAL CONVERSION

It is possible to conduct all subsequent data processing steps with the SDS 9300 computer. However, it is understandably the policy of the computer laboratory only to undertake jobs, other than experimental computer science work, which cannot be accomplished by the school's general purpose computer, IBM 360/67 system. Thus, it is necessary to convert the octal integers output by the SDS 9300 to hexidecimal representation for use by the IBM 360.

This is done using the FORTRAN program 7TO9 listed below. The program is executed in the IBM 360 computer. It is based on a similar program given in Ref. 16.

Logical unit numbers used in all FORTRAN READ and WRITE statements in this thesis are as follows:

2: seven track tape

4: nine track tape

5: card reader

6: Line printer

7: card punch.

The program converts the octal integers to hexadecimal integers, converts these to four byte real numbers, and stores them on a nine track magnetic tape. The actual numerical conversion is accomplished by the assembler language subroutine, FORM, which has been precompiled and resides in the user library, MPSLIB [Ref. 16].

It would be possible to conduct all subsequent data processing steps without re-writing the data on the nine track tape. However, this would approximately double the computer time in operating with the seven track tape. Since there is only one seven track mounting in the IBM 360 system, and several other users, it is advisable to go through the intermediate step of writing the nine track tape. This also facilitates an earlier receipt of portions of the final data processing product, since the nine track tape data can be conveniently processed one file at a time.

The program 7TO9 requires approximately seven minutes CPU time to process five files with NCHAN equal two and NSAMP equal 512, where the files contain 15 seconds of real-time data.

Significant variables in the program are defined below.

NRECL is the total number of samples per record. It must be equal to NSAMP times NCHAN.

FACTOR is an arbitrary constant introduced to provide convenient sized values of the intensity and drive signals for later processing. With the instrument tape recorder output in the range of 1-10 volts during A/D conversion, FACTOR equal to $10.0^{-4}$ produces data values in the range 10.0 to 1000.0, depending on the amplifier settings that are used on the COMCOR 5000 computer. FACTOR equal to $100.0X2.0^{-23}$ will yield the actual voltage at the A/D trunk of the COMCOR 5000.

The arrays IDAT and DAT must be dimensioned to NRECL.

The FORMAT statement 15 must also provide for reading exactly NRECL words, i.e., as written in Appendix I the statement calls for reading

$$8 \times 128 = 1024 = \text{NRECL}$$

samples.

C. COMPUTATION OF BEAM WANDER AND IMAGE SHAPE

Listed below is the FORTRAN program BEAM WANDER/SPREAD, which computes RMS beam wander, time average image shape, and time average image shape with beam wander removed. The main sequences of the program are given in Figure 11 and are shown in detail on Figure 12.

The program consists basically of two nested loops. The outer loop performs operations on each record, and the inner loop operates on each image within the record. The beginning of the inner loop is signified by the box marked branch in Figure 11.

After initializing arrays and variables, the program commences the outer loop by reading the first record from the magnetic tape. It sorts the data so that the image intensity signal is placed in array C1 (for channel 1), and the scan drive signal in channel 2, C2. It then searches for the first

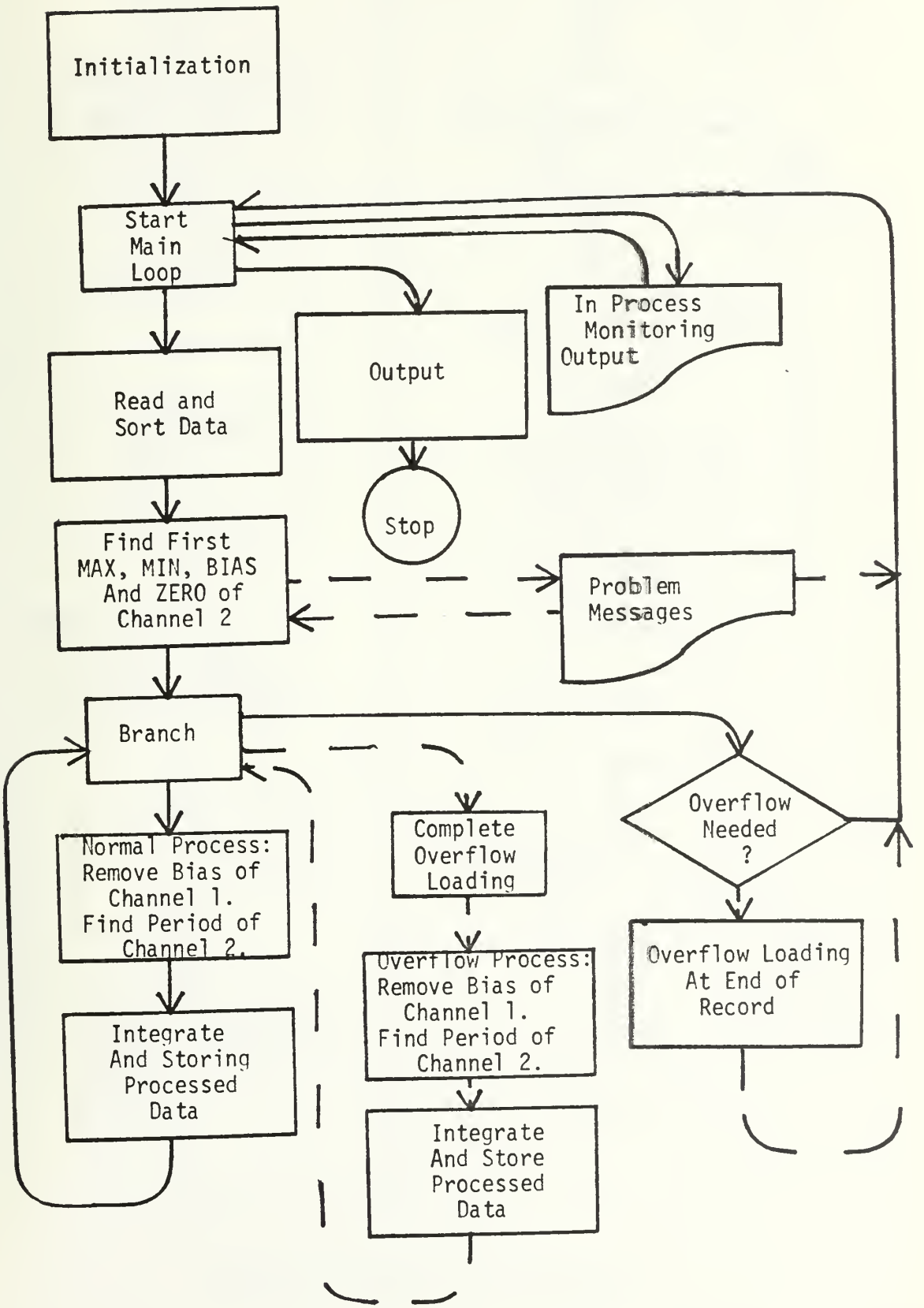


FIGURE 11. Beam Wander/Spread Master Flow Diagram

Initialization and Starting Main Loop

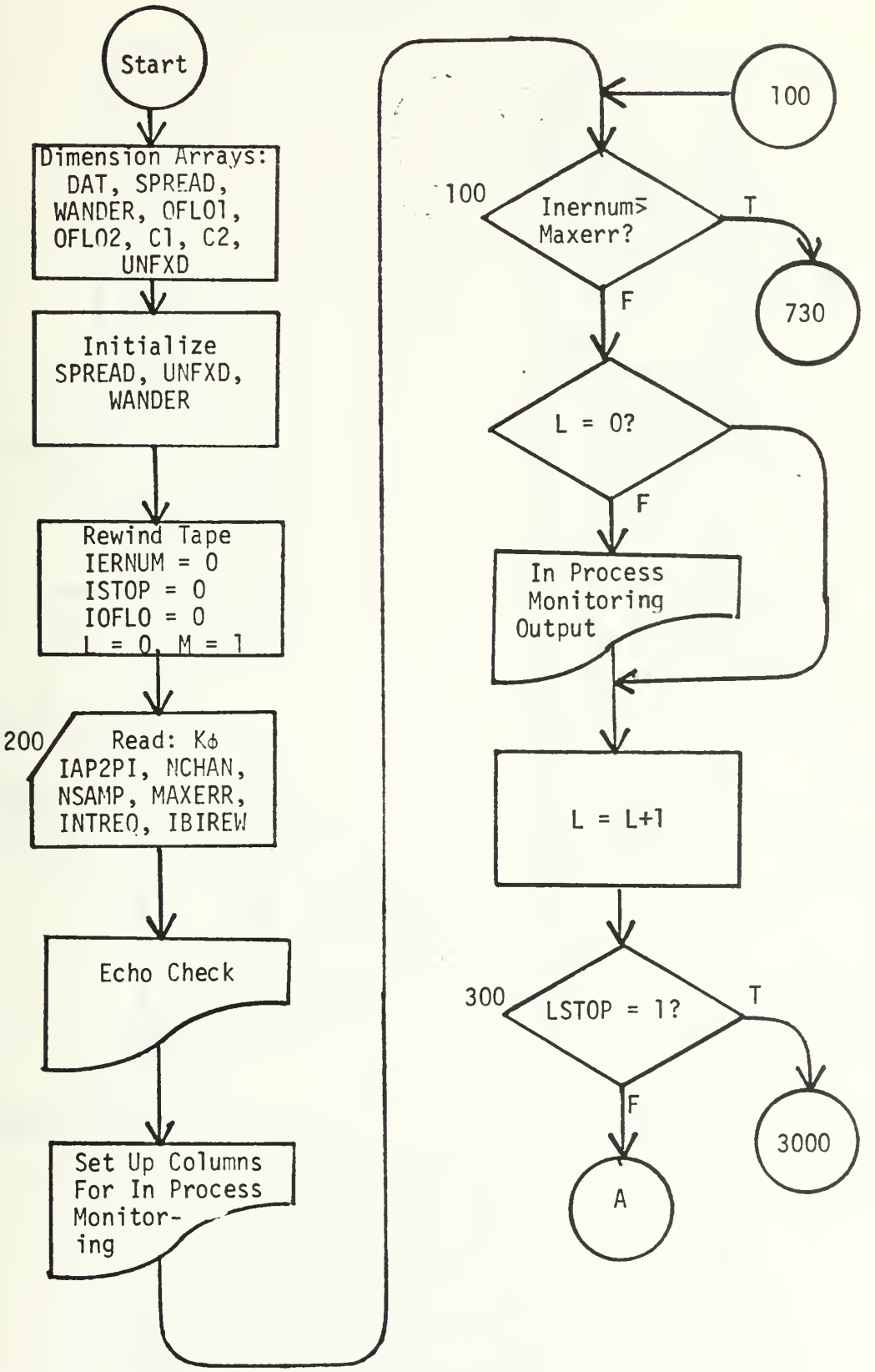


FIGURE 12. Detailed Flow Diagram

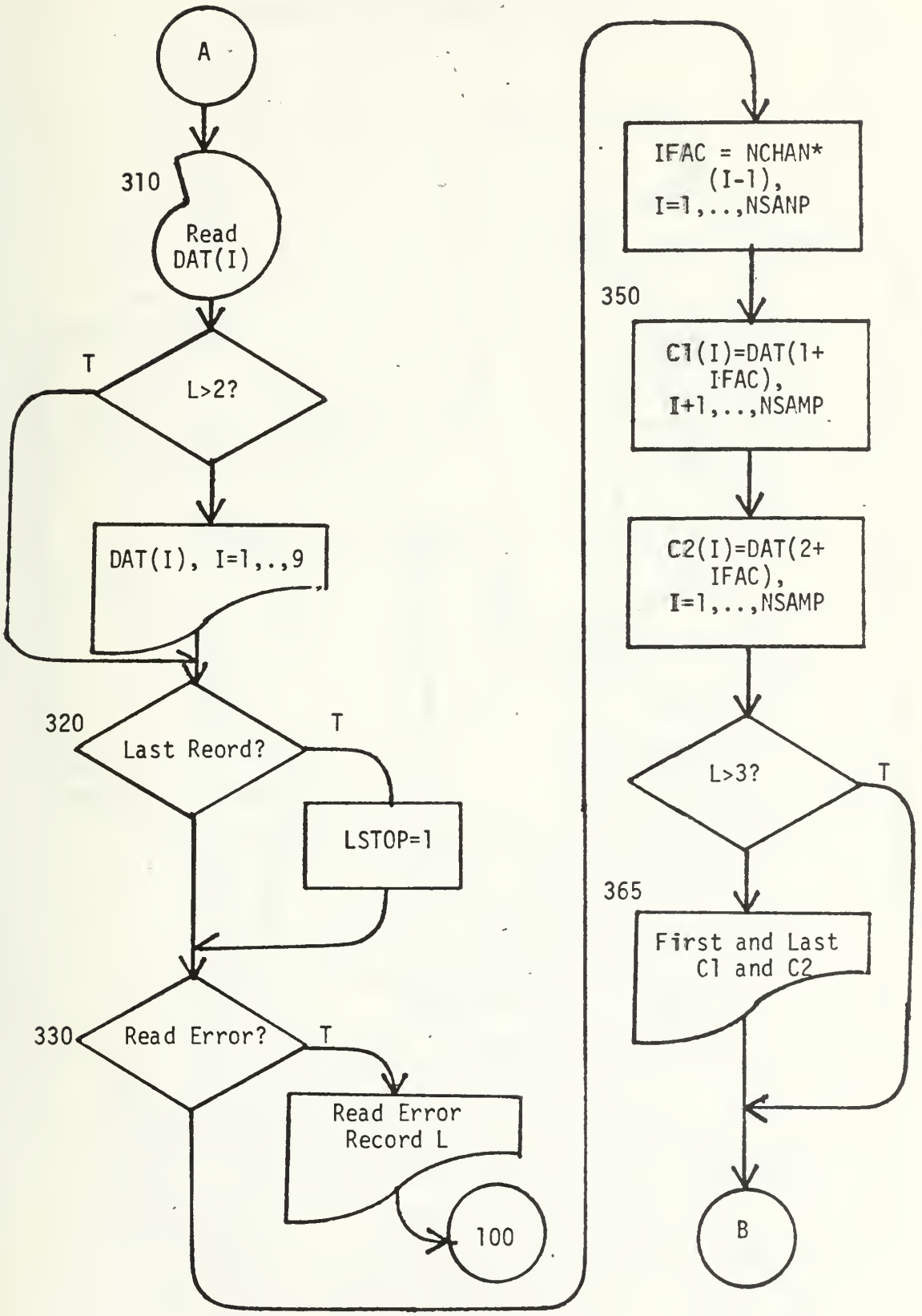


FIGURE 12. Continued

Finding First Maximum of Channel 2

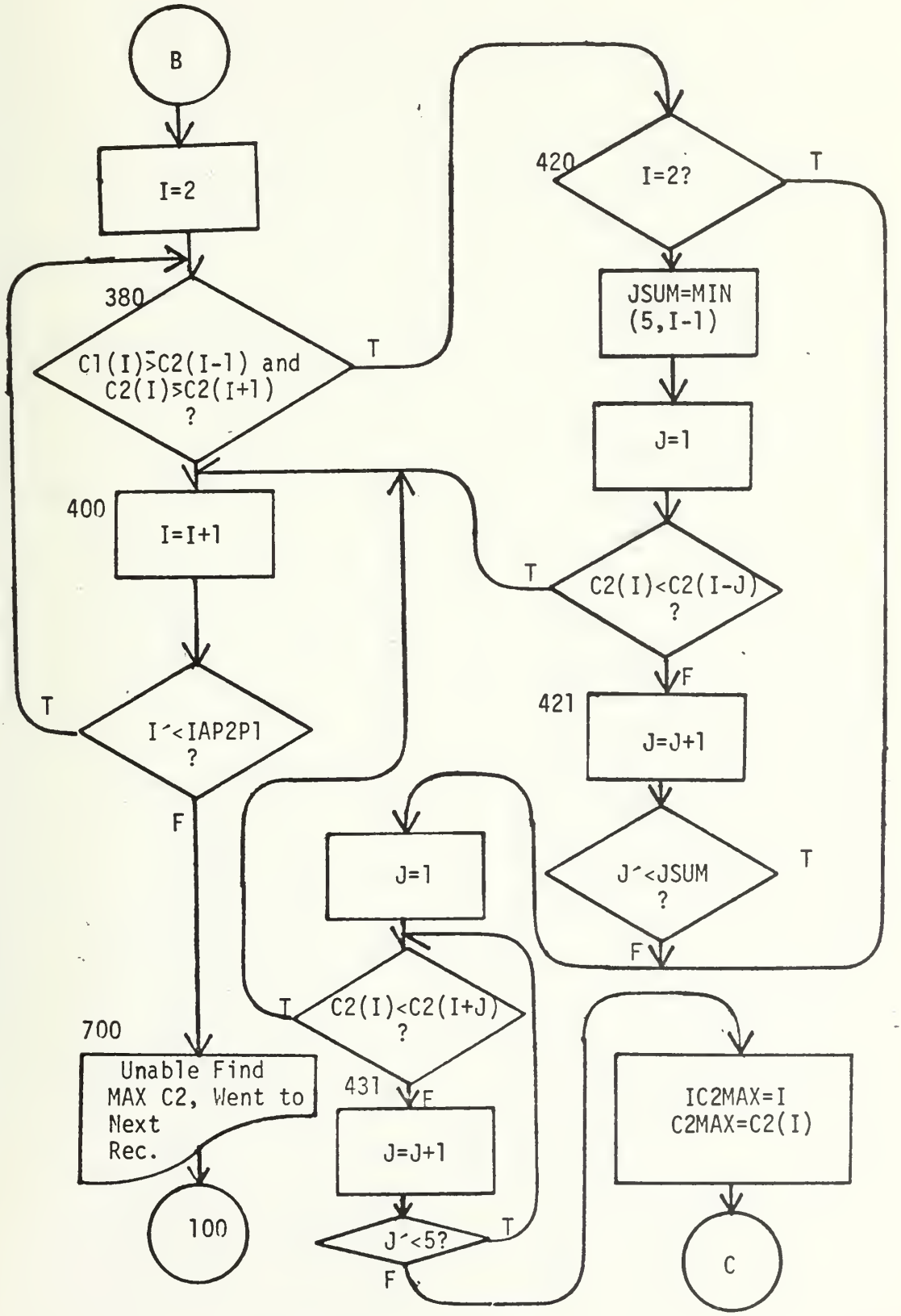


FIGURE 12. Continued

Finding First Minimum of Channel 2

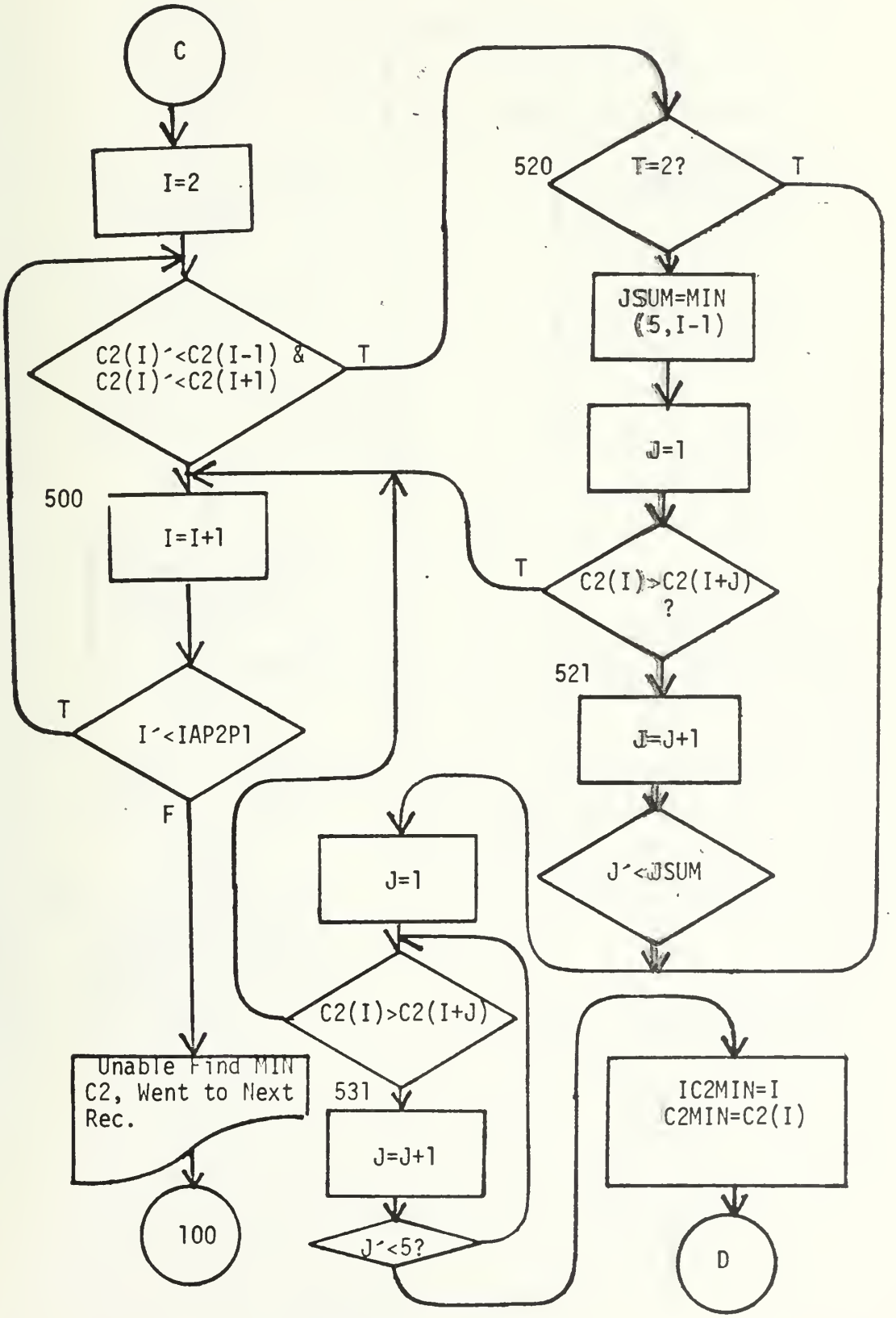


FIGURE 12. Continued

Removing Bias From Channel 2

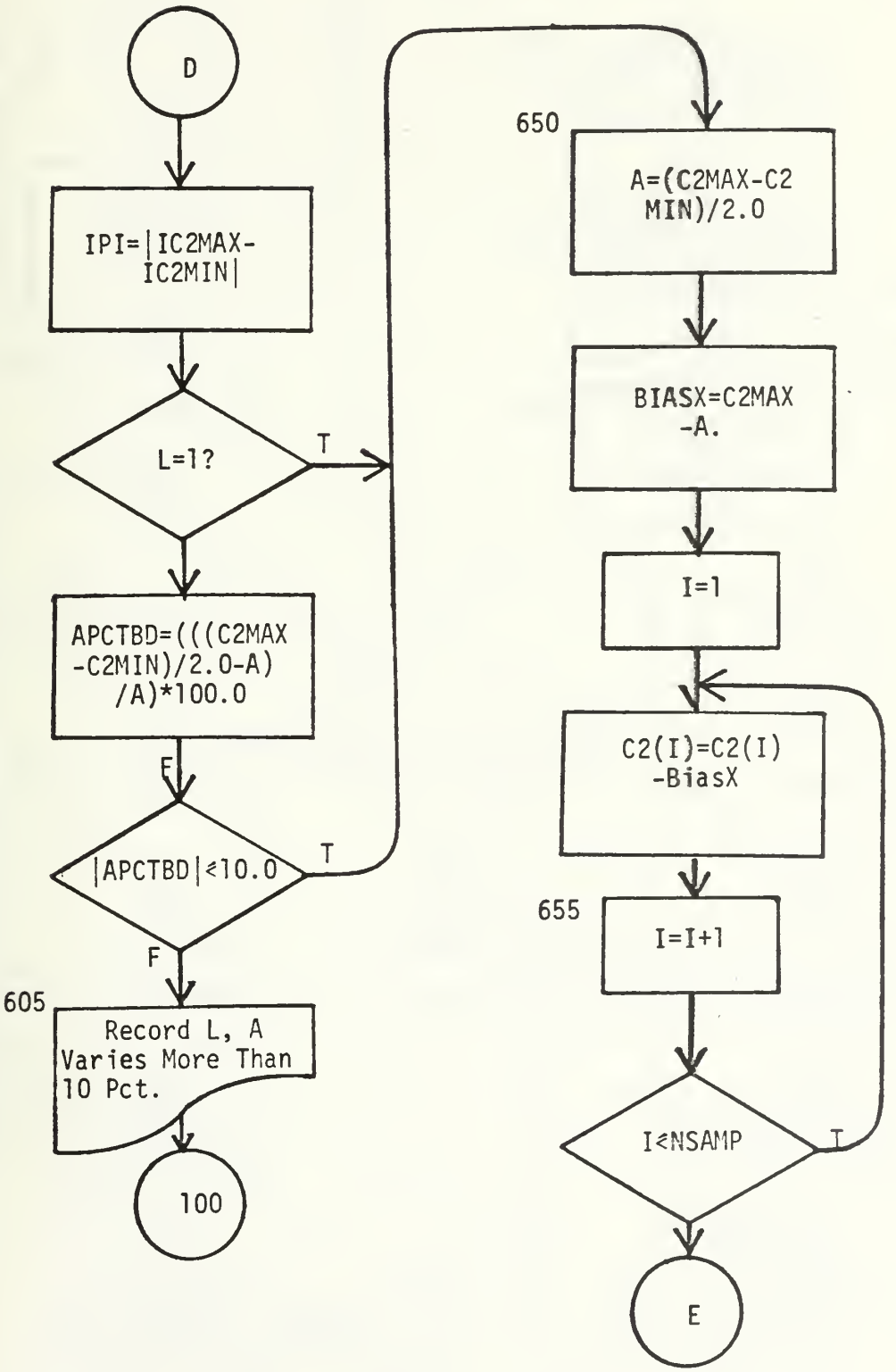


FIGURE 12. Continued

Finding First Zero of Channel 2

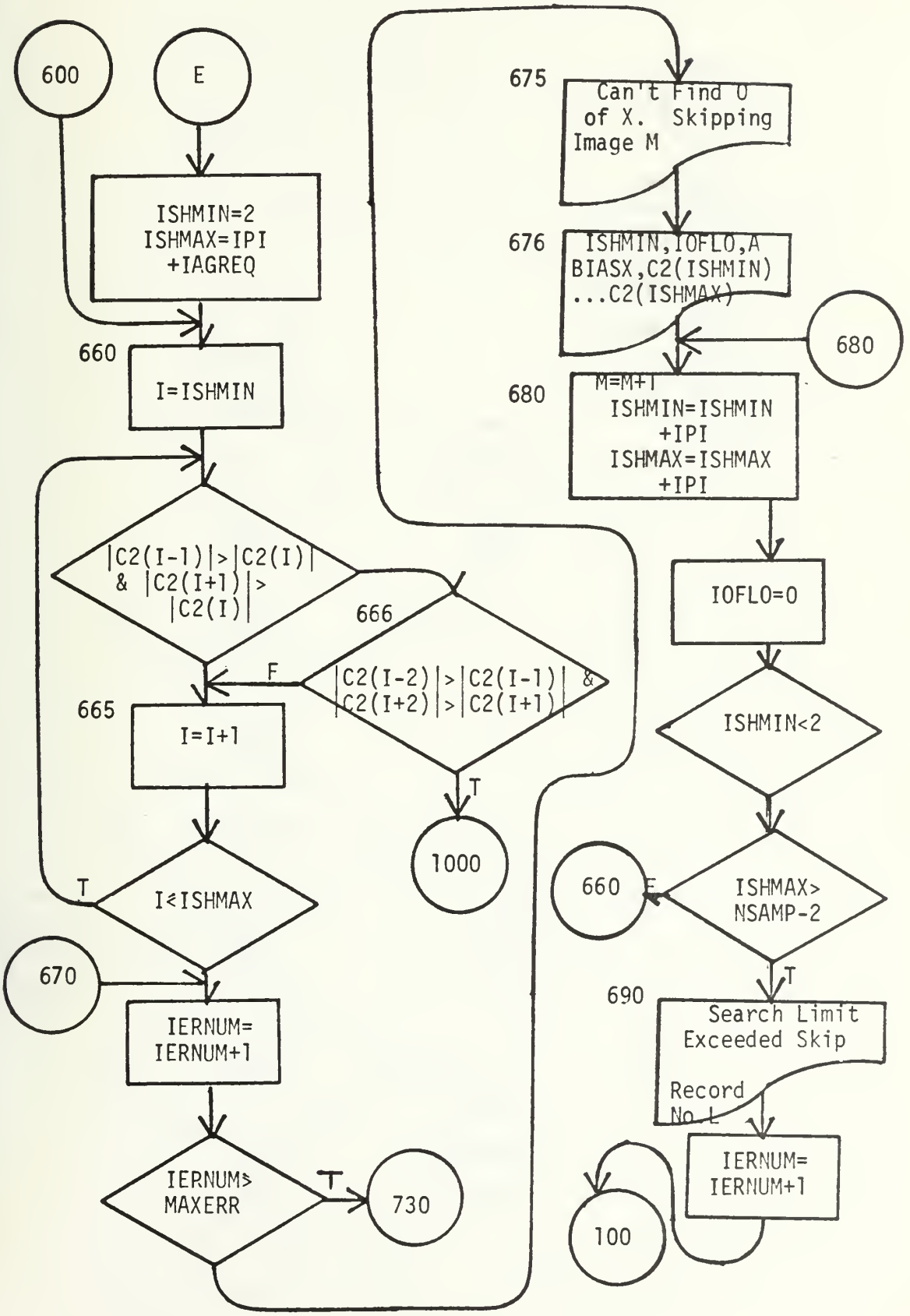


FIGURE 12. Continued

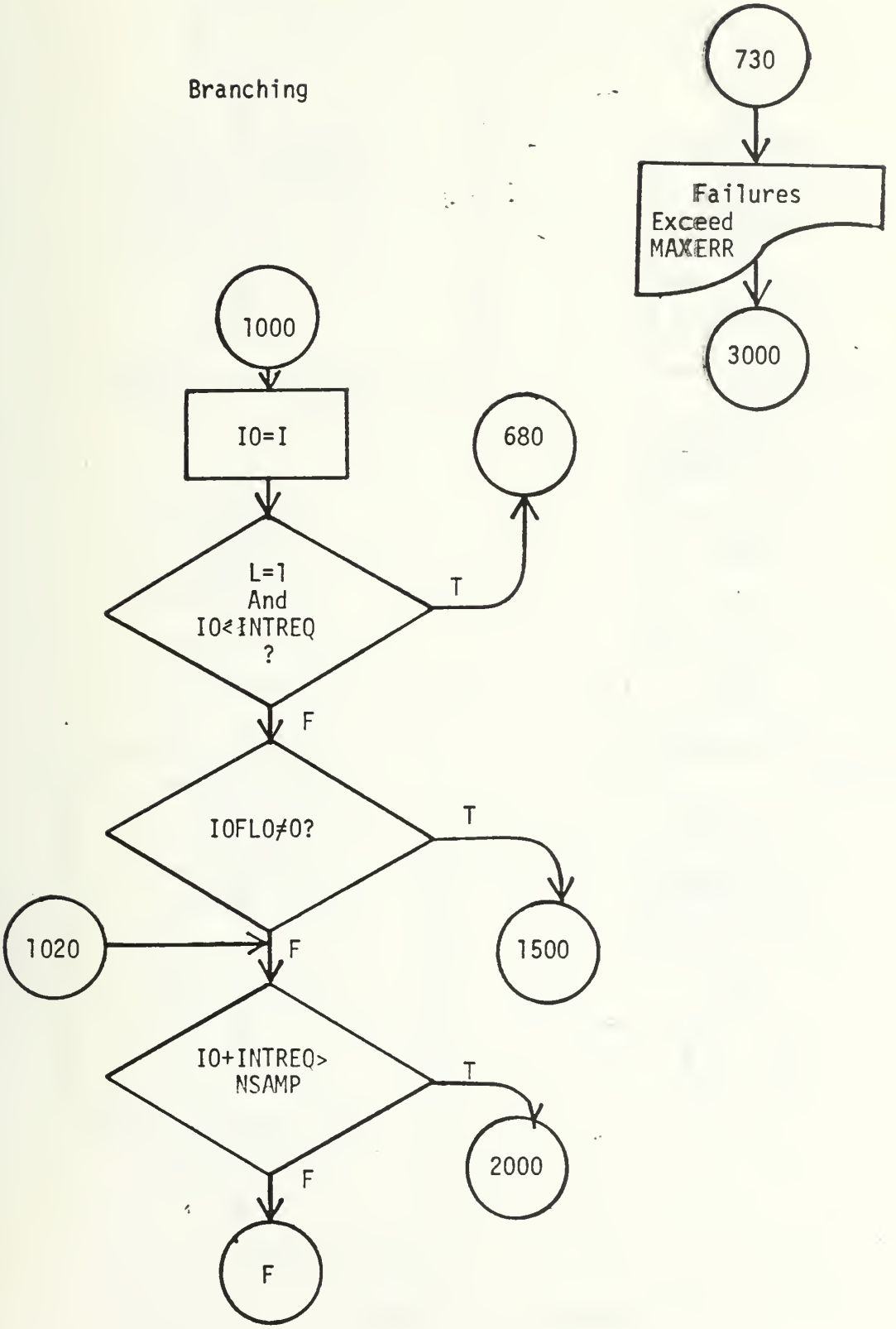


FIGURE 12. Continued

Normal Case: Removing Bias From Channel 1

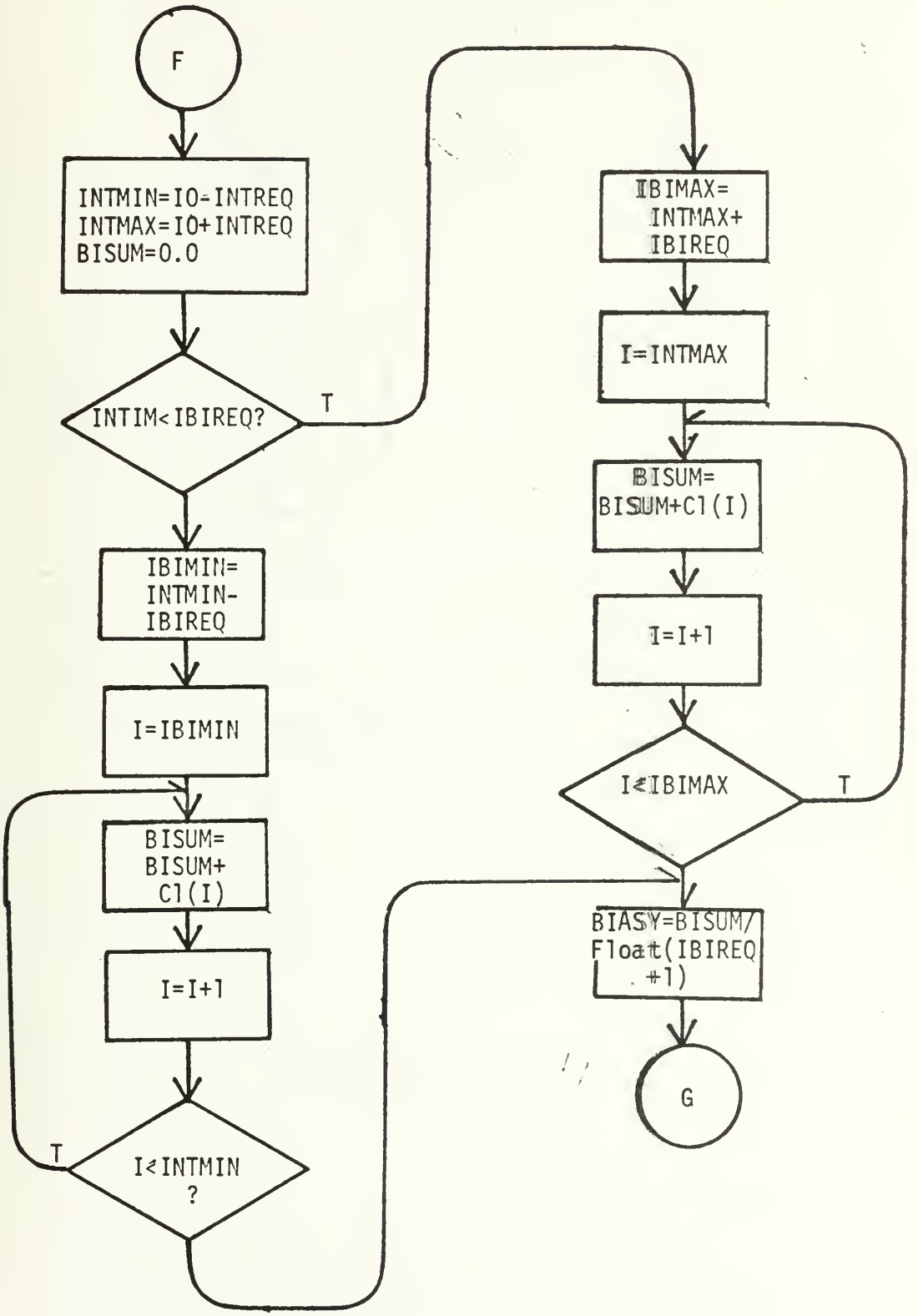


FIGURE 12. Continued

Normal Case: Removing Bias From Channel 1 (Cont.)

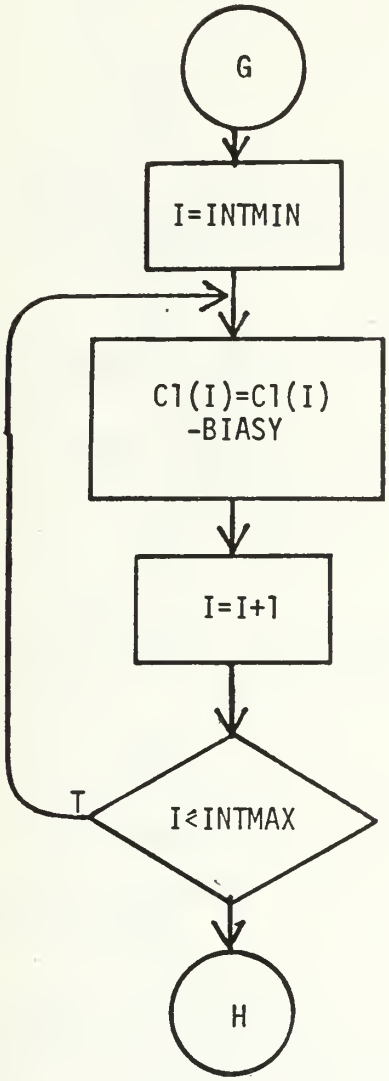


FIGURE 12. Continued

Normal Case: Finding Period of Channel 2

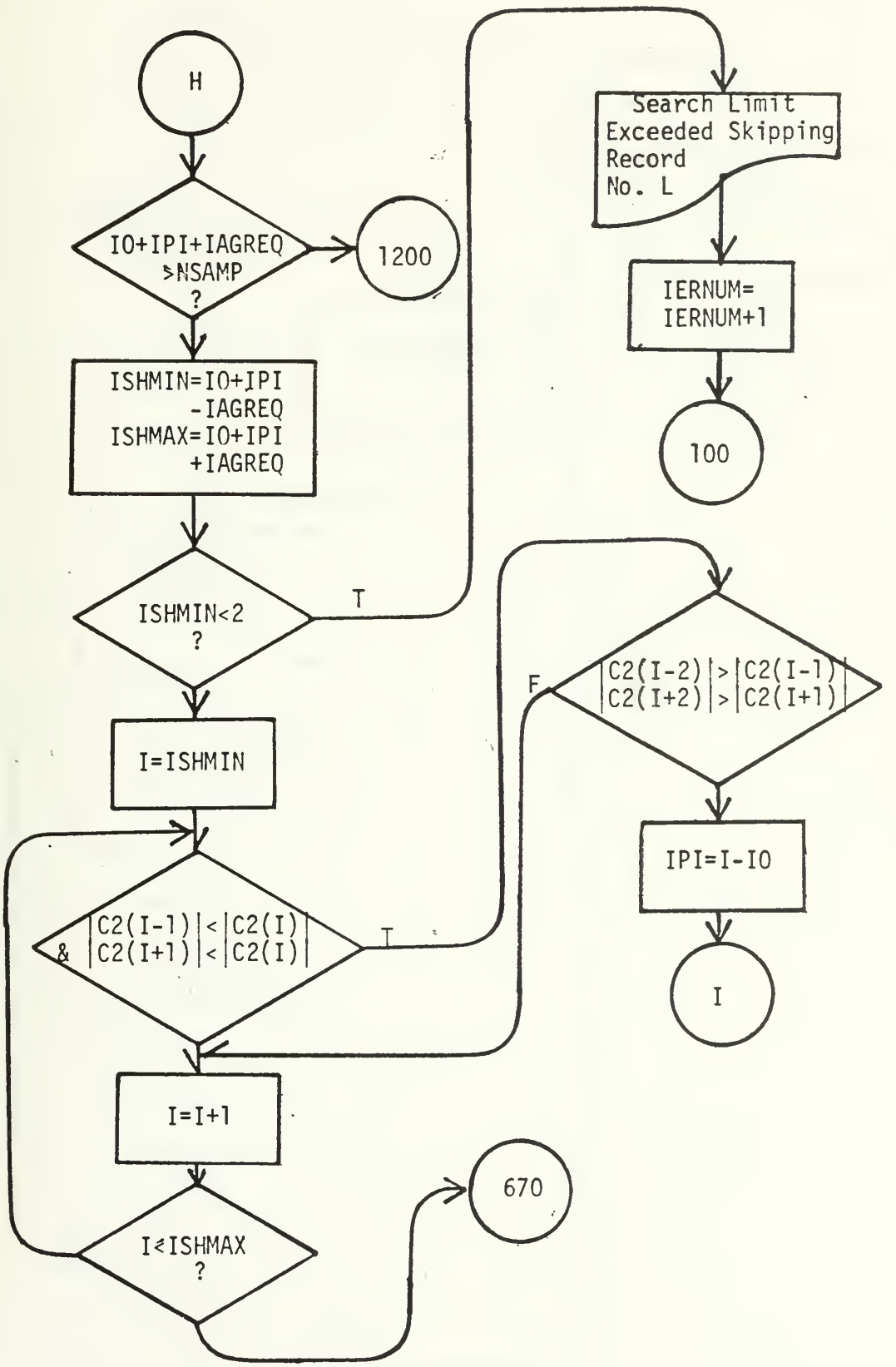


FIGURE 12. Continued

Normal Case Integrations

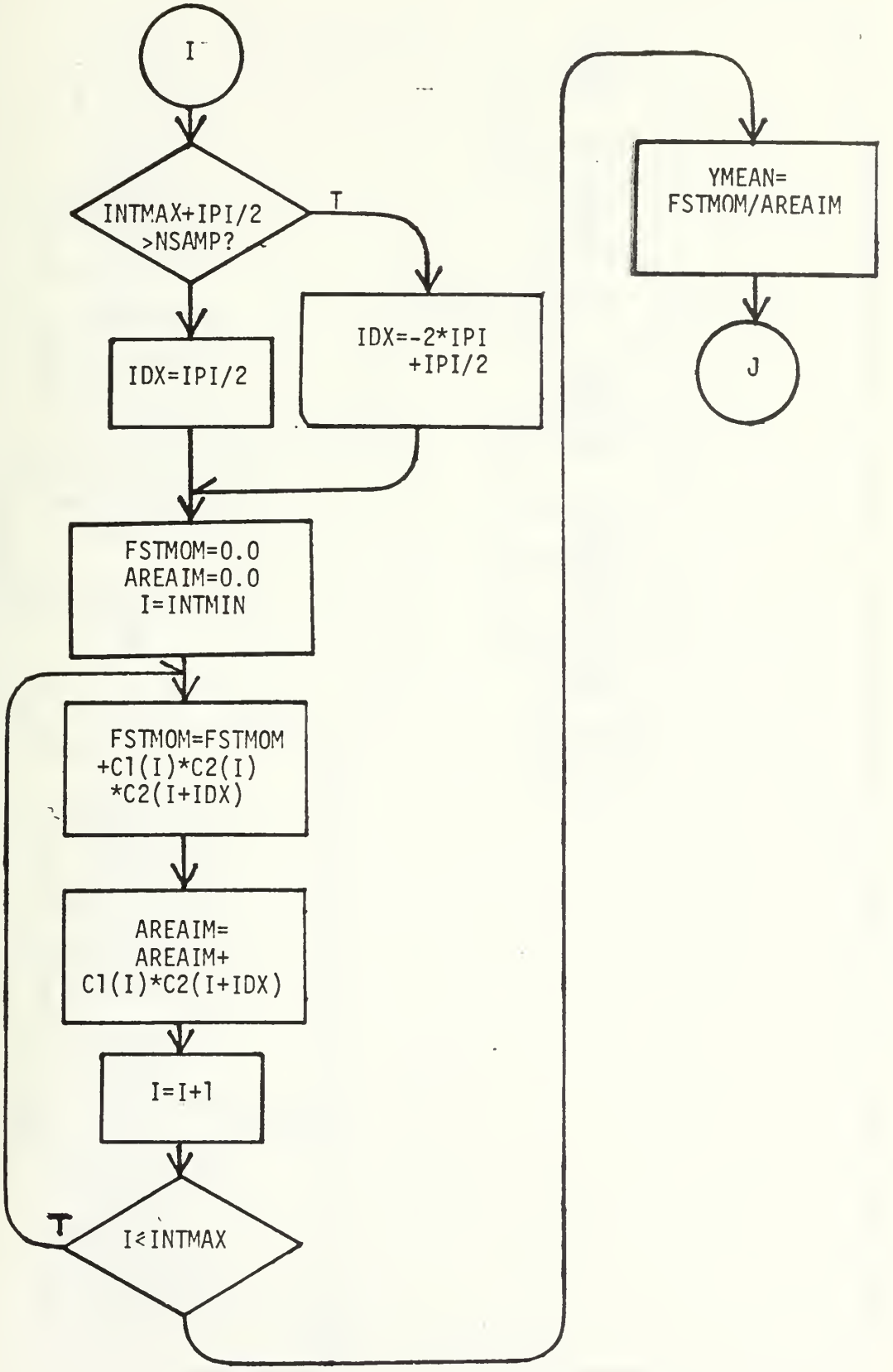


FIGURE 12. Continued

Normal Case: Loading Arrays and Preparing Next Integration Sequence

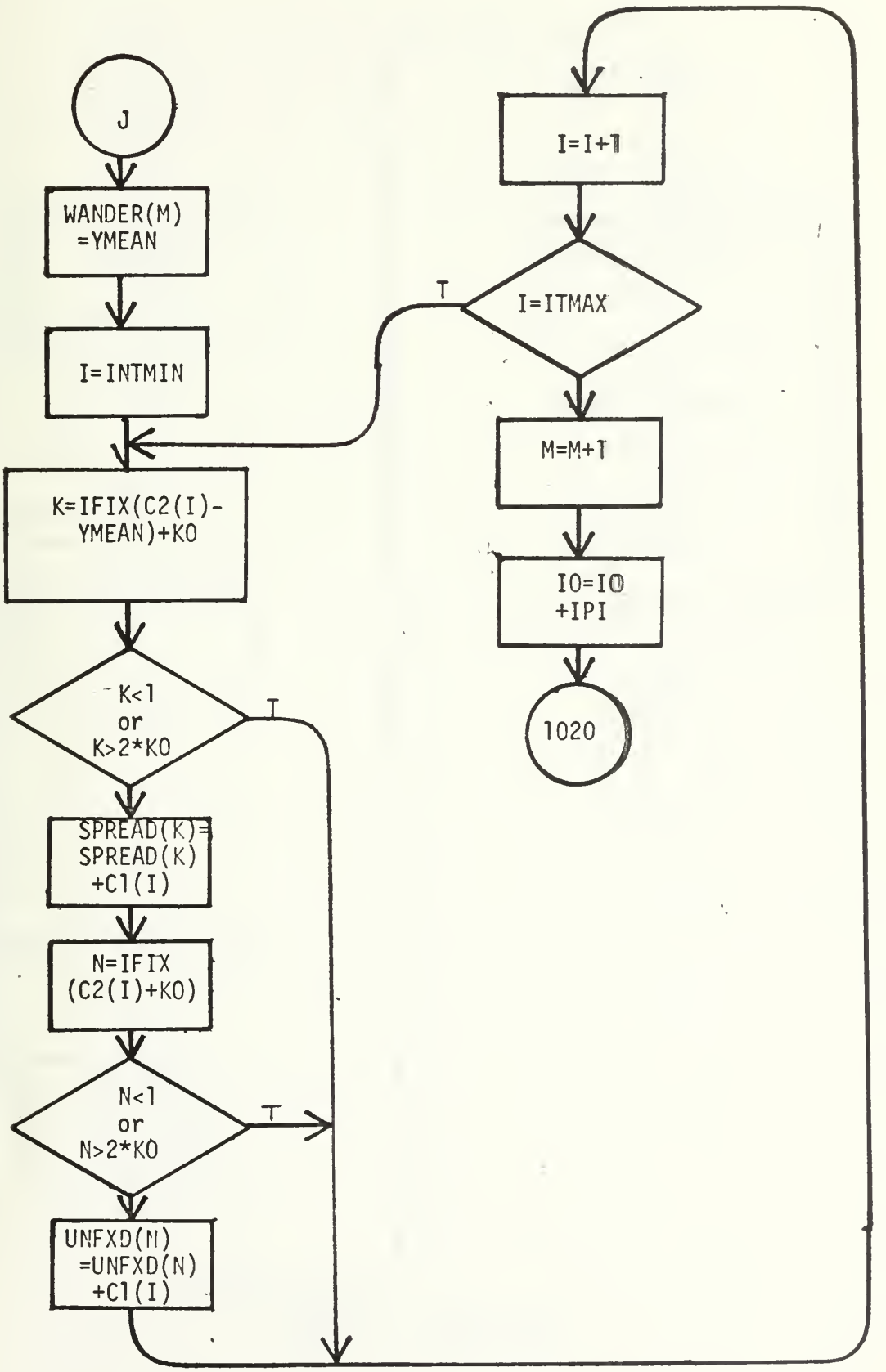


FIGURE 12. Continued

Overflow Case: Loading Overflow

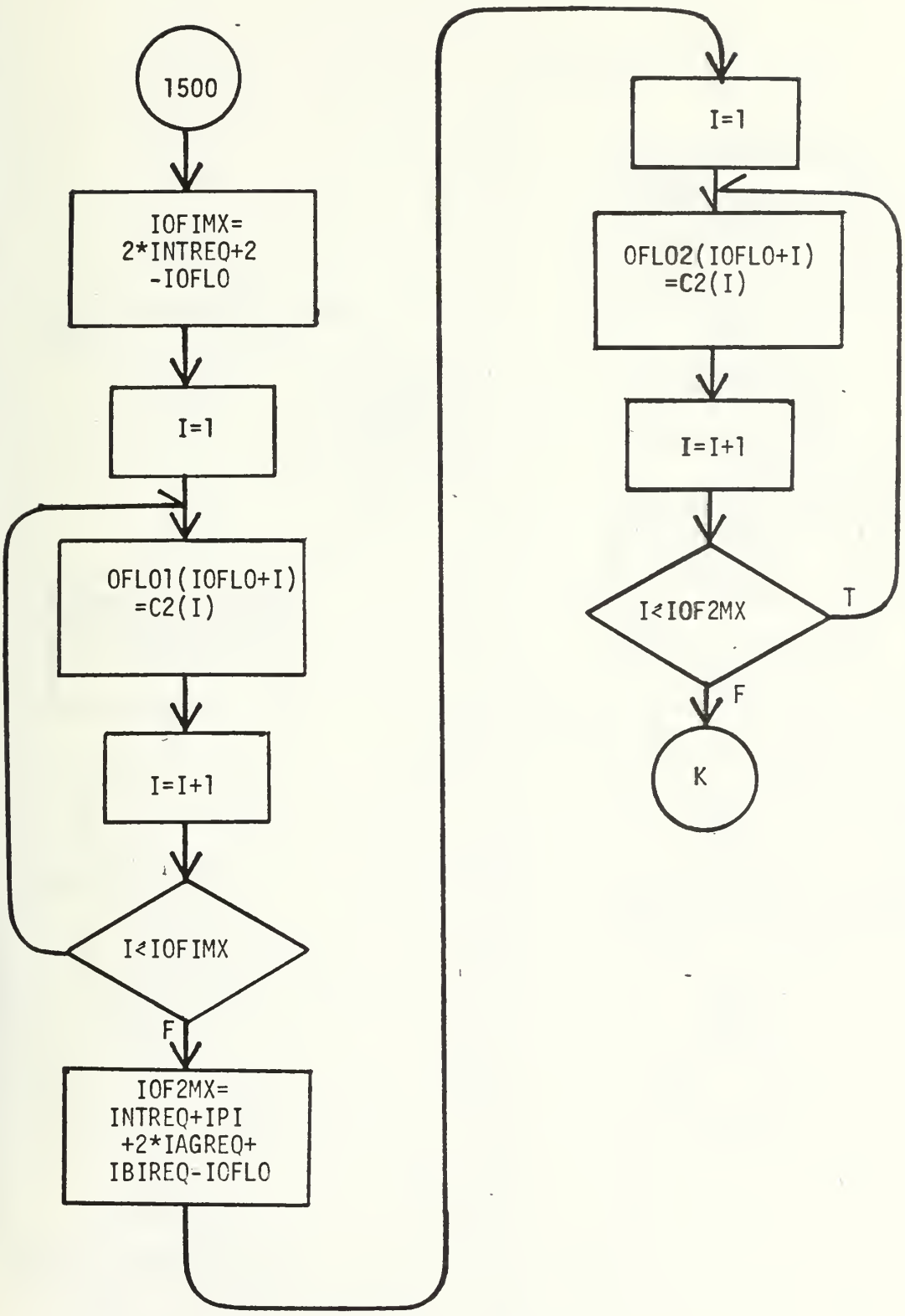


FIGURE 12. Continued

Overflow Case: Removing Bias From Channel 1

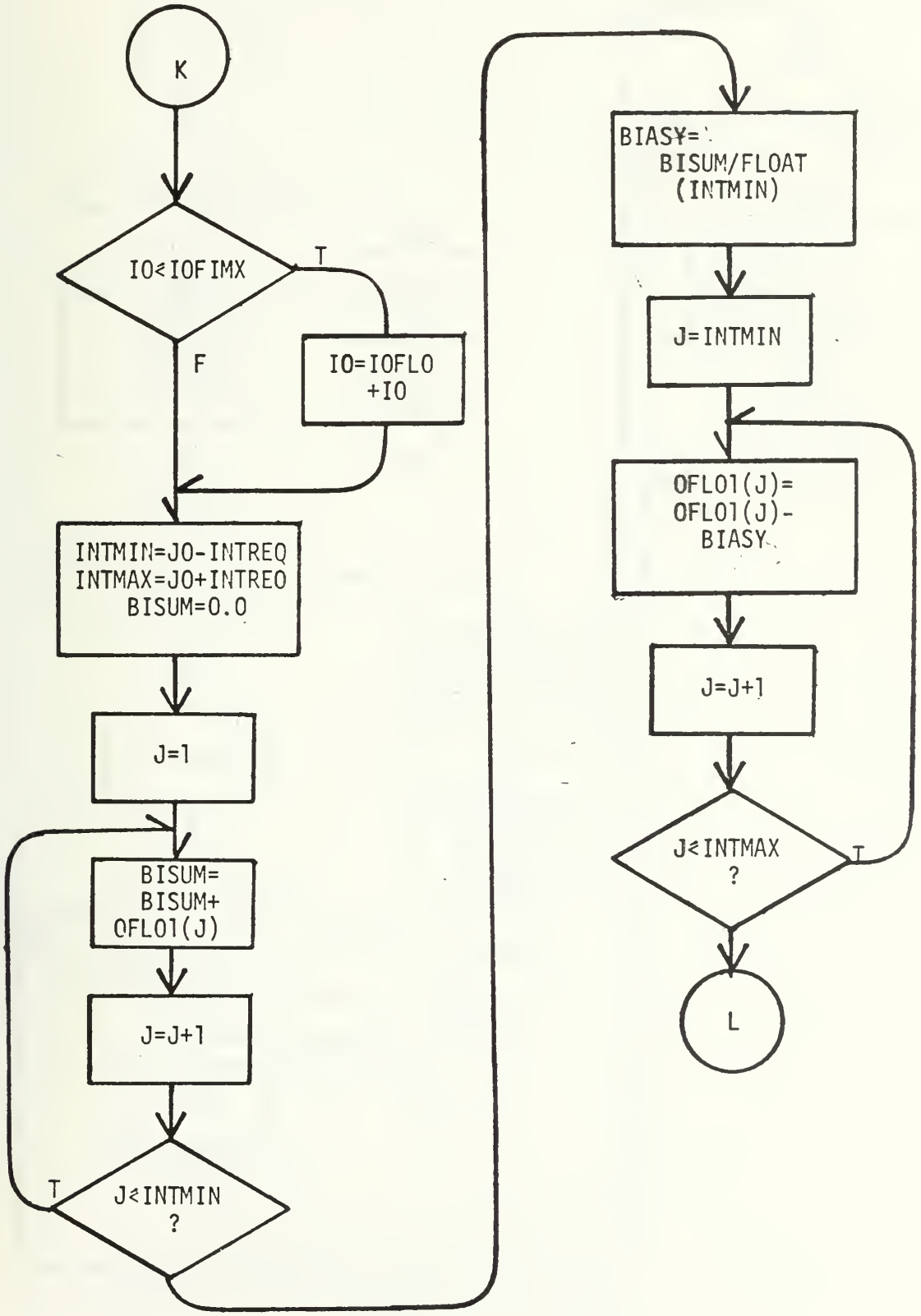


FIGURE 12. Continued

Overflow Case: Finding Period of Channel 2

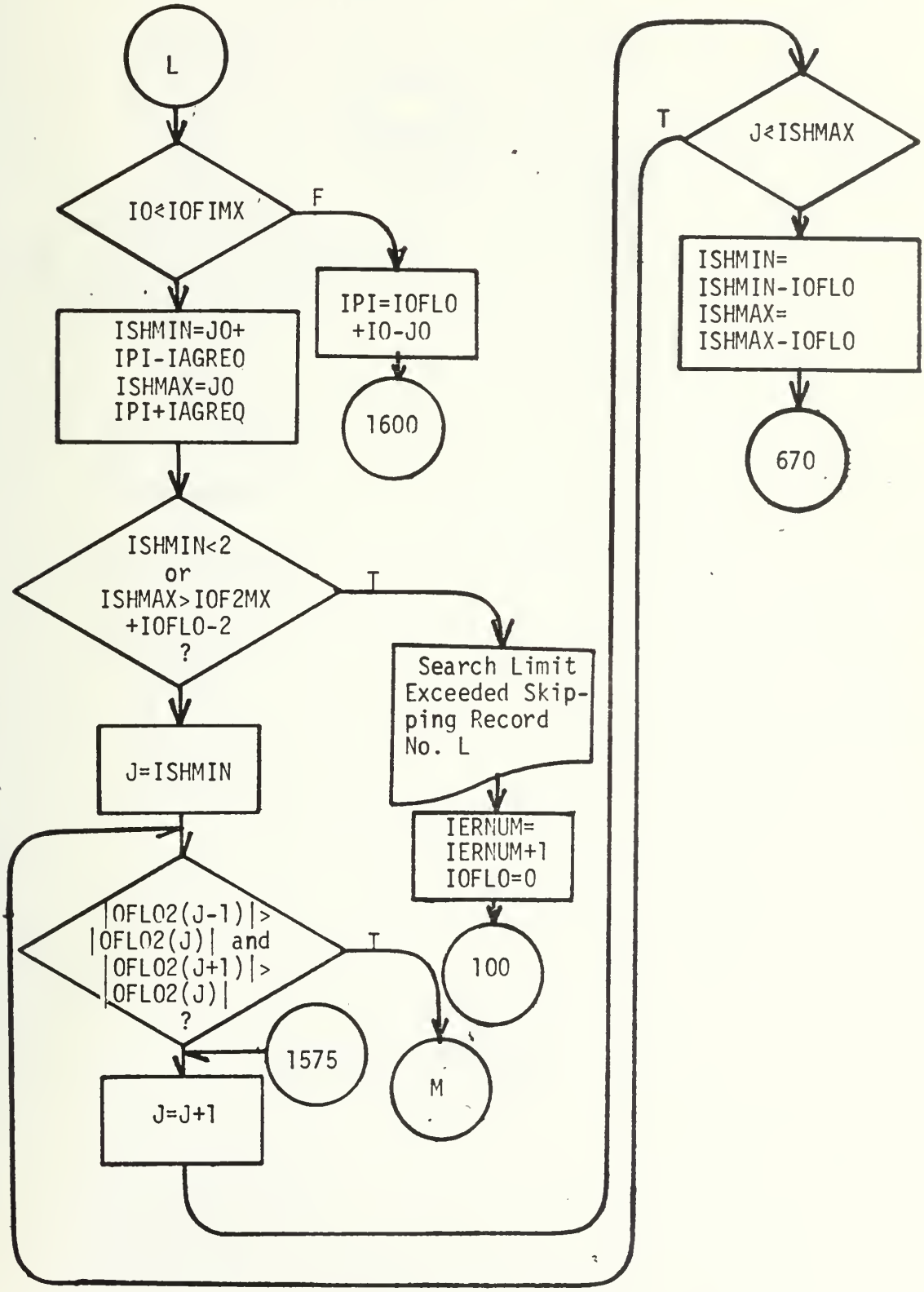


FIGURE 12. Continued

Overflow Case: Finding Period of Channel 2 (Cont.)

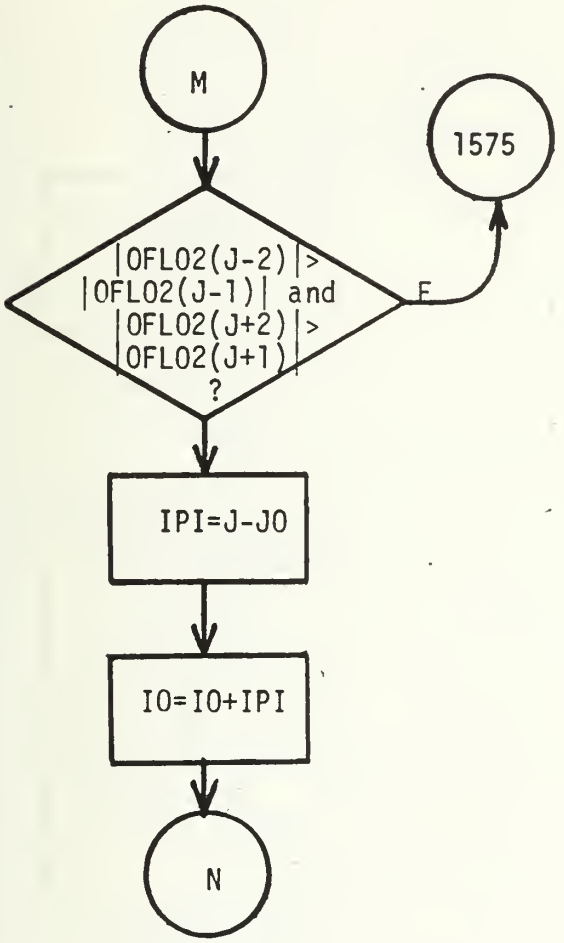


FIGURE 12. Continued

Overflow Case: Integrations

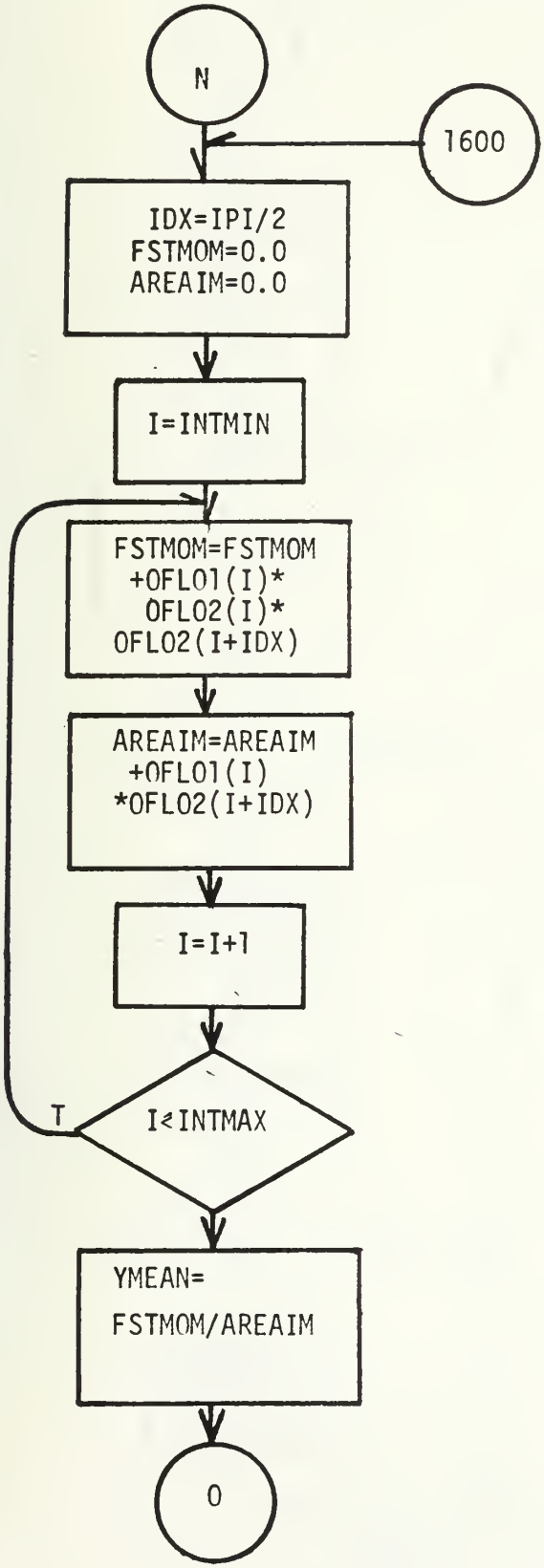


FIGURE 12. Continued

Overflow Case: Loading Arrays and Preparing Next Integration Sequence

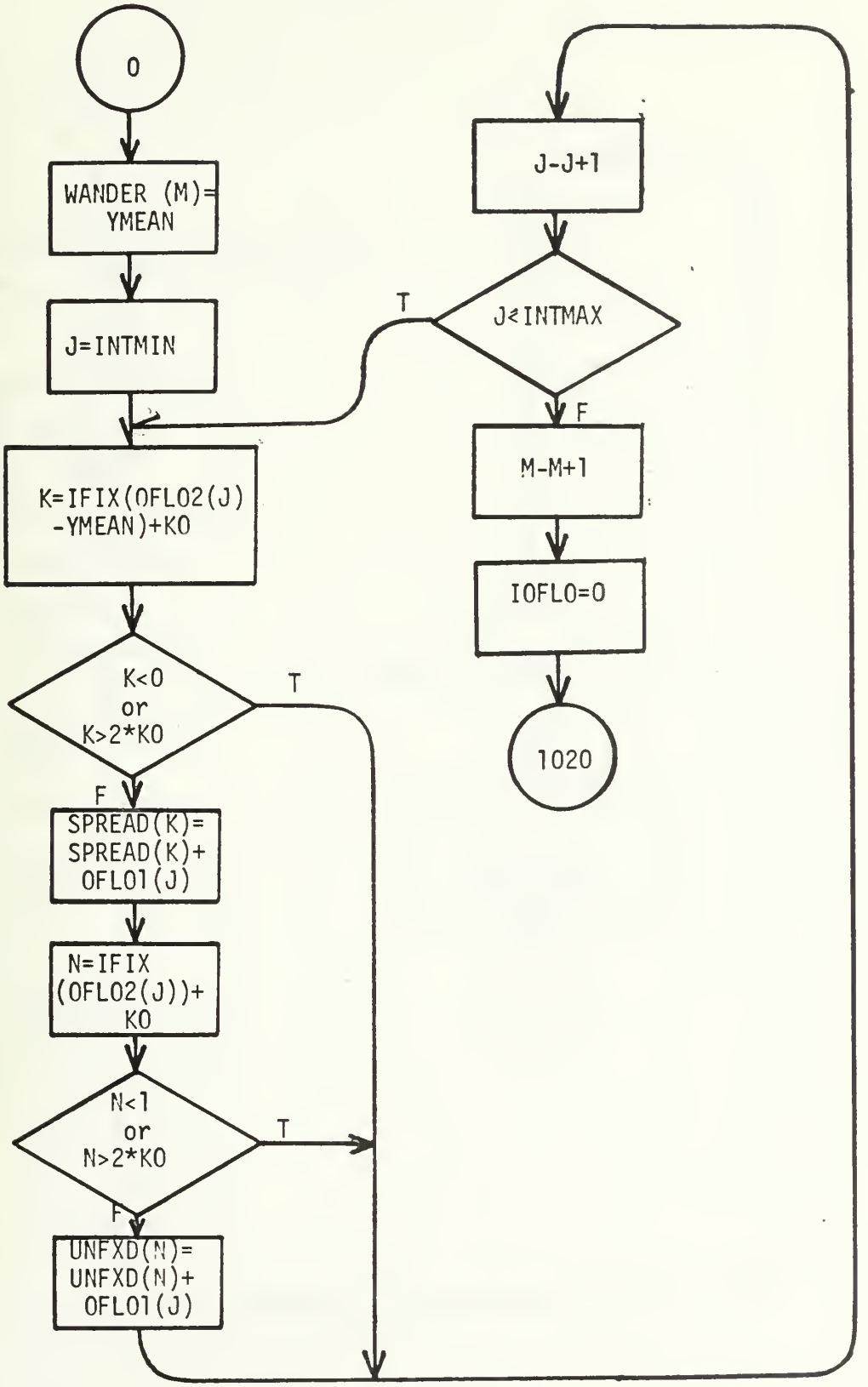


FIGURE 12. Continued

Loading Overflow at End of Record

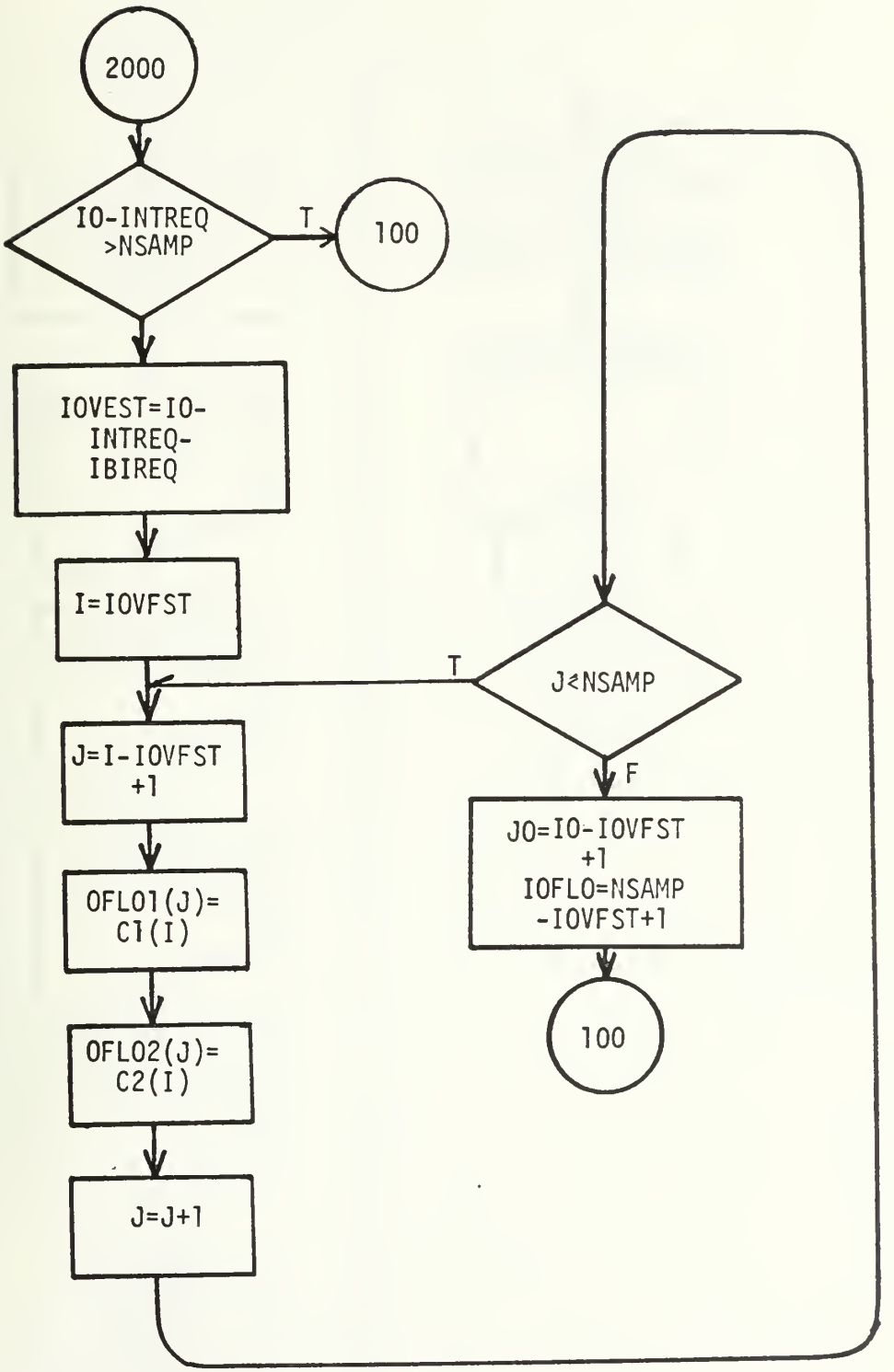


FIGURE 12. Continued

Output

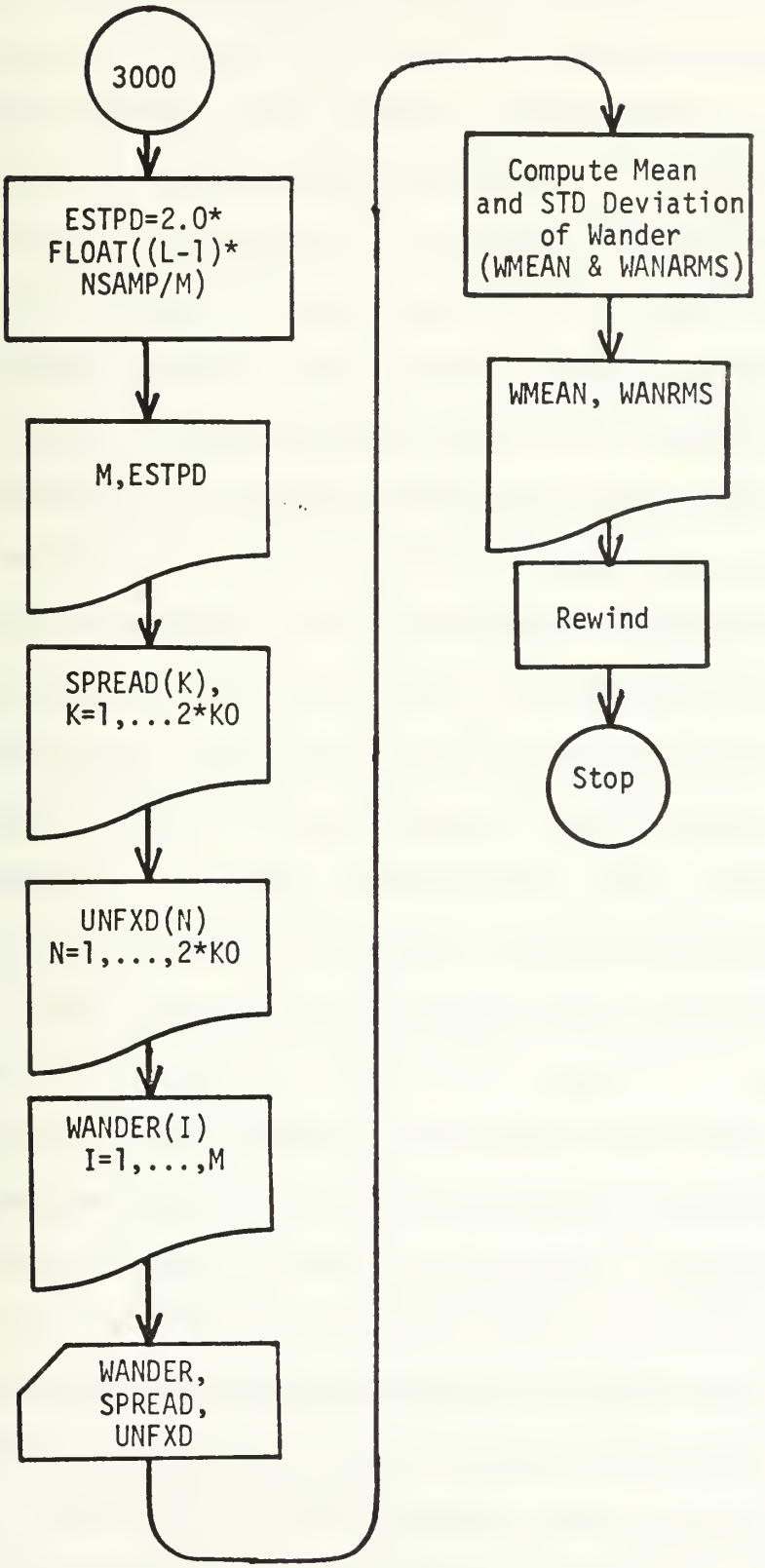


FIGURE 12. Continued

maximum and minimum of C2, and if it finds them it computes the bias of C2 and subtracts it off, leaving a purely A.C. sinusoid. If the program cannot find the maximum or minimum of C2 due to abnormalities in the sine wave, it returns to the start of the loop and reads the next record. Normally this condition doesn't occur, however, and the program continues in the outer loop by finding the first zero of C2. It does this by searching for the smallest absolute value of C2 in a domain slightly larger than a half period of the sinusoid as determined from the points where the first maximum and minimum appeared. Again, this is normally successful; however, if it is not, the program advances another half period and searches again. At the branch point, the program determines whether there are any samples in the overflow arrays OFL01 and OFL02. These arrays are filled at the end of a record if the domain of C1 required for the integrations described below overlaps the end of the record. At the beginning of a record, if there are values in these arrays, the program completes the loading of them and conducts the inner loop operations on the first image using OLF01 and OFL02 instead of C1 and C2. All subsequent images in the record are processed using the values in C1 and C2. The inner loop operations are as follows. First the bias of C1 is removed over a domain immediately before the domain of integration. Both of these domains have length specified by the user during initialization. The center of the domain of integration is always the same location as the zero of C2 found previously. After removing the bias from C1 over the domain of integration, the program searches for the next zero of C2. The difference between the current zero and the next zero is taken as a more accurate value of the half period, since C2 is a more rapidly changing function near its zeros than near its maximum or minimum. This value of the half period is then used in approximating the derivative of C2 for use in the integration sequence. The integration

sequence, which computes the centroid of the image intensity relative to the zero of C2, is described in detail in section 2 below. After this computation the program stores the position of the centroid in the array WANDER. The position of the centroid is then subtracted from the position of each intensity sample in the image and the samples are added to the array SPREAD. Each image is added to SPREAD with its centroid at the mid-point of the array. Thus, SPREAD accumulates a time average image shape with beam wander removed. In a similar way, but without subtracting the position of the controid, the program adds the intensity samples from the image to the array UNFXD to accumulate a time average image shape with beam wander included. Having completed these operations, the program advances to the next zero of C2 and returns to the beginning of the inner loop. It checks whether there is sufficient room left on the record to recycle through the loop. If there isn't, it checks whether the end of the record falls within the integration region of the next image, as described above. If not, the program returns to the beginning of the outer loop immediately. However, if the end of the record falls within the integration domain, the program loads the overflow arrays from the beginning of the bias removal domain to the end of the record and then returns to the beginning of the outer loop.

When the end of the file is reached, the program branches to the output sequence. Here it outputs the values stored in WANDER, SPREAD, and UNFXD to the line printer as well as to punched cards for later processing.

If desired, another loop can be added encircling both the loops described above to allow processing of more than one file at a time. This has been done successfully with some of the data processed, but is not included here in order not to unnecessarily complicate the description. The start and stop points for such a loop are immediately after the first REWIND

statement and before the last REWIND statement, respectively. If used, this procedure requires DO loops to re-initialize SPREAD, WANDER, and UNFXD at the beginning of each file.

1. Initialization

The initialization sequence dimensions arrays, reads input parameters, rewinds the tape to the beginning of the file specified by the Job Control Language (JCL) statements submitted with the job [Ref. 17], and initializes the counting parameters defined below.

L is the current record number being processed.

M is the sequential number of the image being processed.

IOFLO is the number of data points loaded into overflow arrays OFL01 and OFL02 at the end of a record to provide continuity at the beginning of the next record.

IERNUM is the number of times the program has failed to find a zero, maximum or minimum of the scan drive signal (channel 2).

Variables which must be input via the card reader are as follows.

IAP2PI is the approximate number of samples in one period of the scan drive signal. This may be estimated either from the sample rate used when digitizing the data or from the printed output of 7T09.

NCHAN and NSAMP are as defined above.

MAXERR is an upper bound on IERNUM. If IERNUM reaches this value the program automatically goes to the output sequence.

INTREQ is the half width of the integration domain to be used in computing the centroid of each image, expressed as a number of samples. Its value can be chosen by refering either to the 7T09 printout or a dual trace display of both channels to determine an upper bound on the fraction of the period of channel 2 required for the image signal to rise from and return to its D.C. level. The integration is carried out from $I_0$-INTREQ to $I_0$+INTREQ,

where $I_0$ is such that $C2(I_0)$ is nearest to zero for each image. In this regard it should be noted that the scan drive signal is phase shifted during the digitizing process to correspond to the phase of the deflection of the scanning mirror, so that images are entered in the data stream near each zero of channel 2.

IBIREQ is the number of samples of the intensity (channel 1) required to determine the bias of channel 1 at each image.

IAGREQ is the allowable variation in the length of half a period of channel 2, expressed as a number of samples.

KO is the mid-point of the arrays used to accumulate time average image shape and time average image shape with beam wander removed.

All arrays provided are one dimensional. Their functions and dimensions required are described below.

DAT stores all the data from each record. It must have exactly the same dimension as was used for DAT in 7T09.

SPREAD and UNFXD store the time average image shape with wander removed and time average image shape without wander removed respectively as they accumulate. The points in SPREAD and UNFXD are in the spatial rather than the time reference frame. That is, they are the nearest integer to the value of channel 2. Thus, they should be dimensioned to correspond to whatever fraction of the amplitude of channel 2 will contain the entirity of each image. For example, suppose either from observing the original tape recording or the printed output of 7T09, it is determined that every image occurs within $\pi/8$ of the zeroes of channel 2, and that from the 7T09 printout it is determined that channel 2 varies from -100 to 100. Then SPREAD and UNFXD should be dimensioned to at least $2 \times 100 \sin \pi/8$. In general it is possible to dimension these arrays larger than one would ever need, and not worry about them thereafter, since they are small arrays anyway.

WANDER stores the position of the centroid of each image, and should be dimensioned as large as the number of images in the file.

C1 and C2 contain the values of channel 1 and channel 2 after they have been sorted out in DAT. They should be dimensioned to dim(DAT)/NCHAN.

OFLO1 and OFLO2 are loaded at the end of a record and the beginning of the next record if the end of the record falls within the integration domain. In order to conduct all the operations required in these overflow arrays, OFLO1 must be dimensioned to at least 2 X INTREQ + IBIREQ + 1, and OFLO2 must be at least as large as INTREQ + IAP2PI/2 + 2 X IAGREQ + IBIREQ + 2.

2. Integration Sequences

In order to process the data as quickly as possible, an extremely low order integration process has been used. In fact the method used is actually simply the summing of a histogram. It is felt that this does not add appreciably to the error of the final output, however, due to the relatively small number of sample points in any image which the frequency response of the original data recording process allows. If a much slower scan rate or a much higher frequency response were possible, then a higher order integration process, for example any of the Newton Cotes methods [Ref. 18], might be used.

The integration process linearizes the reference frame in which beam wander and image shape are represented by including the factor C2(I+IDX), where IDX is approximately equal to a quarter period of C2. That is, letting x represent C2 and y represent C1,

$$x = \sin\omega t = \sin\pi I/IPI.$$

$$dx/di = (\pi/IPI)\cdot COS\pi I/IPI = (\pi/IPI)\cdot\sin(\pi I/IPI+IPI/2)$$

$$= (\pi/IPI)\cdot x(I+IDX).$$

Thus,

$$\frac{\Sigma C1(I)C2(I)C2(I+IDX)}{\Sigma C1(I)C2(I+IDX)} \simeq \frac{\int x\cdot y\cdot(dx/dI)\cdot dI}{\int y\cdot(dx/dI)\cdot dI} = \frac{\int x\cdot y\ dx}{\int y\ dx} \quad .$$

### 3. CPU Time and Output

WANDER/SPREAD requires about 1 minute 30 seconds of CPU time and outputs approximately 350 punched cards for a 15 second interval of data collection with a scan rate of 120 images/second.

D. GRAPHICAL OUTPUT

Given below is BEAD, a program which plots time average image shape with and without beam wander, and three intervals of beam wander. The duration of these intervals is one second with the program configured as shown. The variables WCAL and SCAL scale the values of beam wander and the abscissa of the image plot. They are determined from the fraction of the scan drive signal in the distance between diffraction maxima generated by the calibration grid described above, and from the amplitude of channel 2 taken from either the printed output of WANDER/SPREAD or 7T09. TCAL is a factor to scale the graph of beam wander to 1 second.

This program is based almost entirely on Ref. 19, which explains the various subroutines called by the program. Figures 13, 14, and 15 show typical graphs plotted by this program.

E. FREQUENCY ANALYSIS

The program, BEAT, shown below, takes the Fourier transform of the beam wander, using the library subroutine RHARM. RHARM is not precompiled and must be requested in the Job Control Statements submitted with the program. It is based on the Cooley-Tukey algorithm [Ref. 20], and is suitable for processing a set with a large number of data points. Figure 16 shows a typical frequency spectrum plotted by the program.

F. INSTRUMENTAL AND COMPUTATIONAL ERROR

As can be seen from Figure 13, a strong 60 cycle jitter is introduced by either the apparatus or the method of data processing. Which of these factors is the primary cause is not known, since all the data was taken using the scan rate of 60 Hz. In either case the magnitude of this jitter is a convenient measure of the overall data collection and reduction process error.

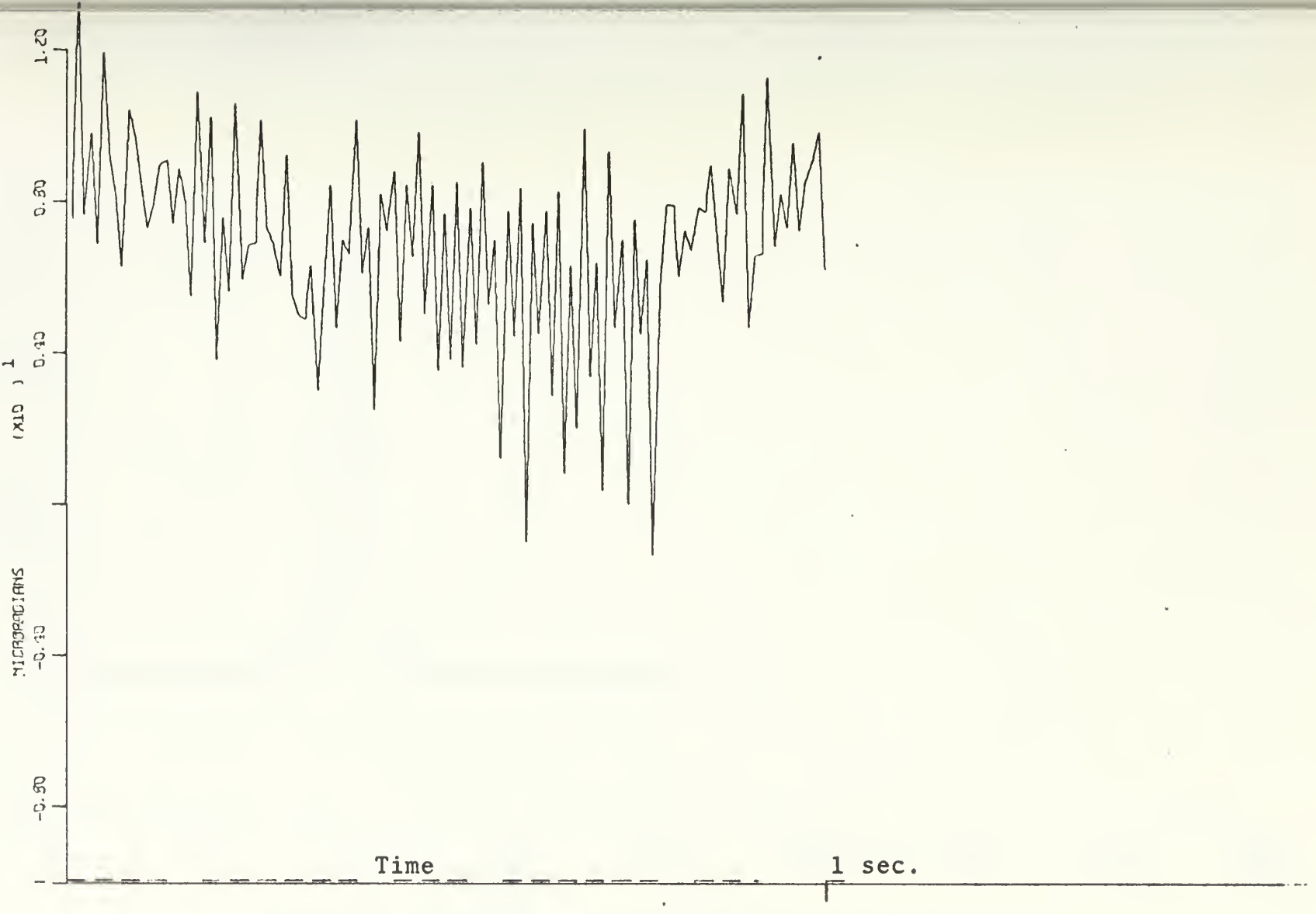


FIGURE 13. Typical Plot of One-Second of Beam Wander

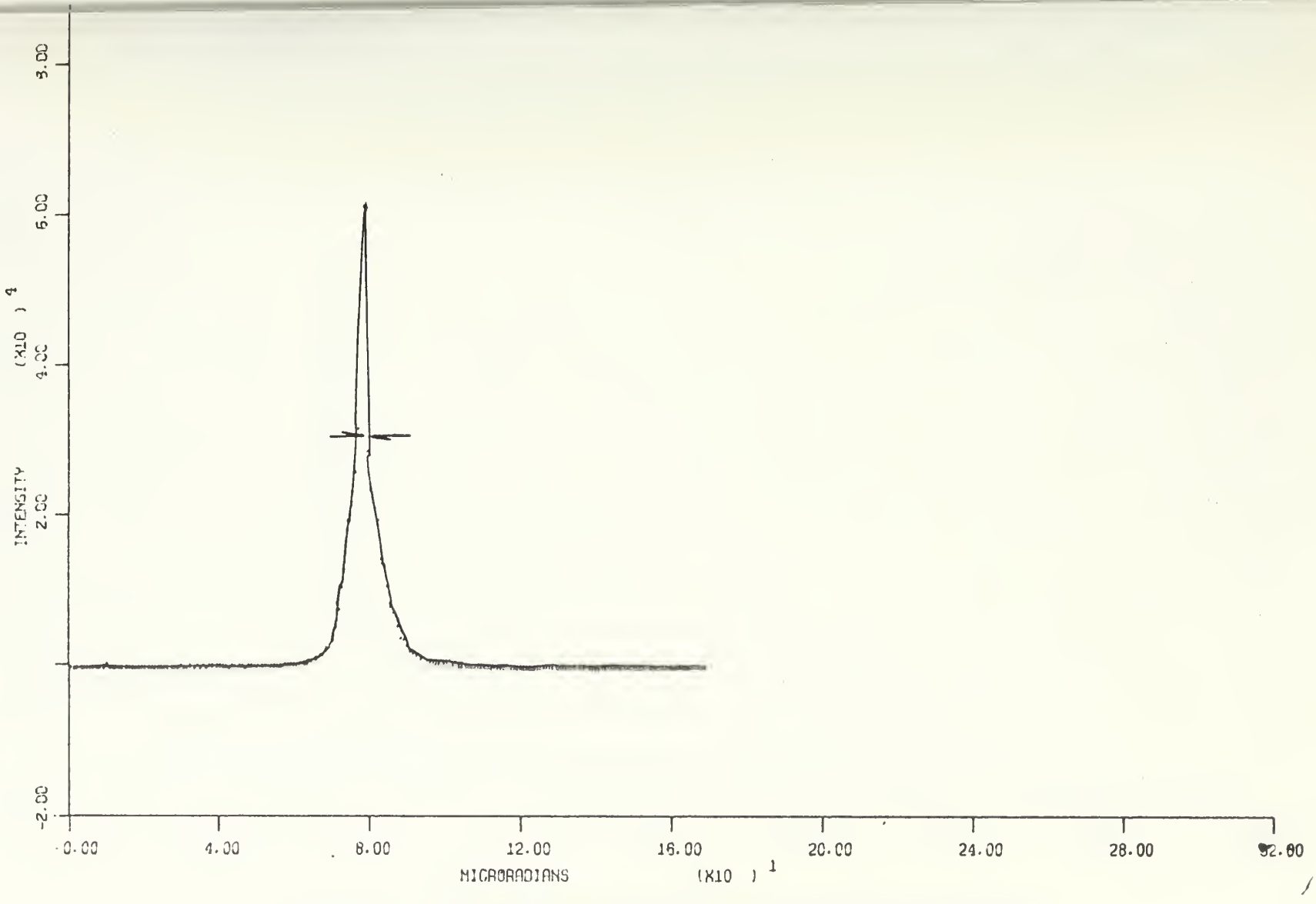


FIGURE 14. Typical Image Shape. Half-Width = 2 Microradians

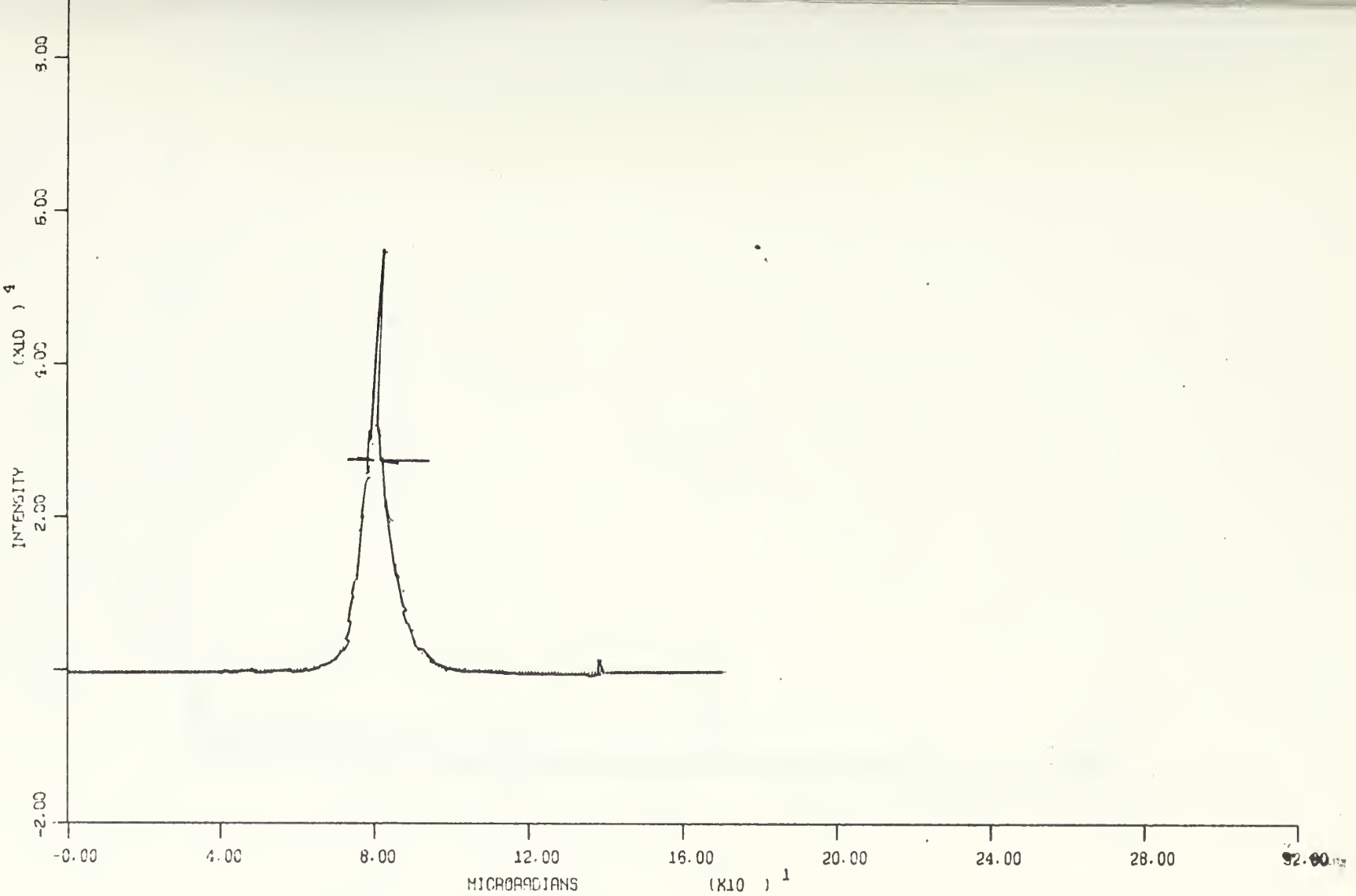


FIGURE 15. Typical Image Shape Without Beam Wander Removed.
Half-Width = 2 Microradians

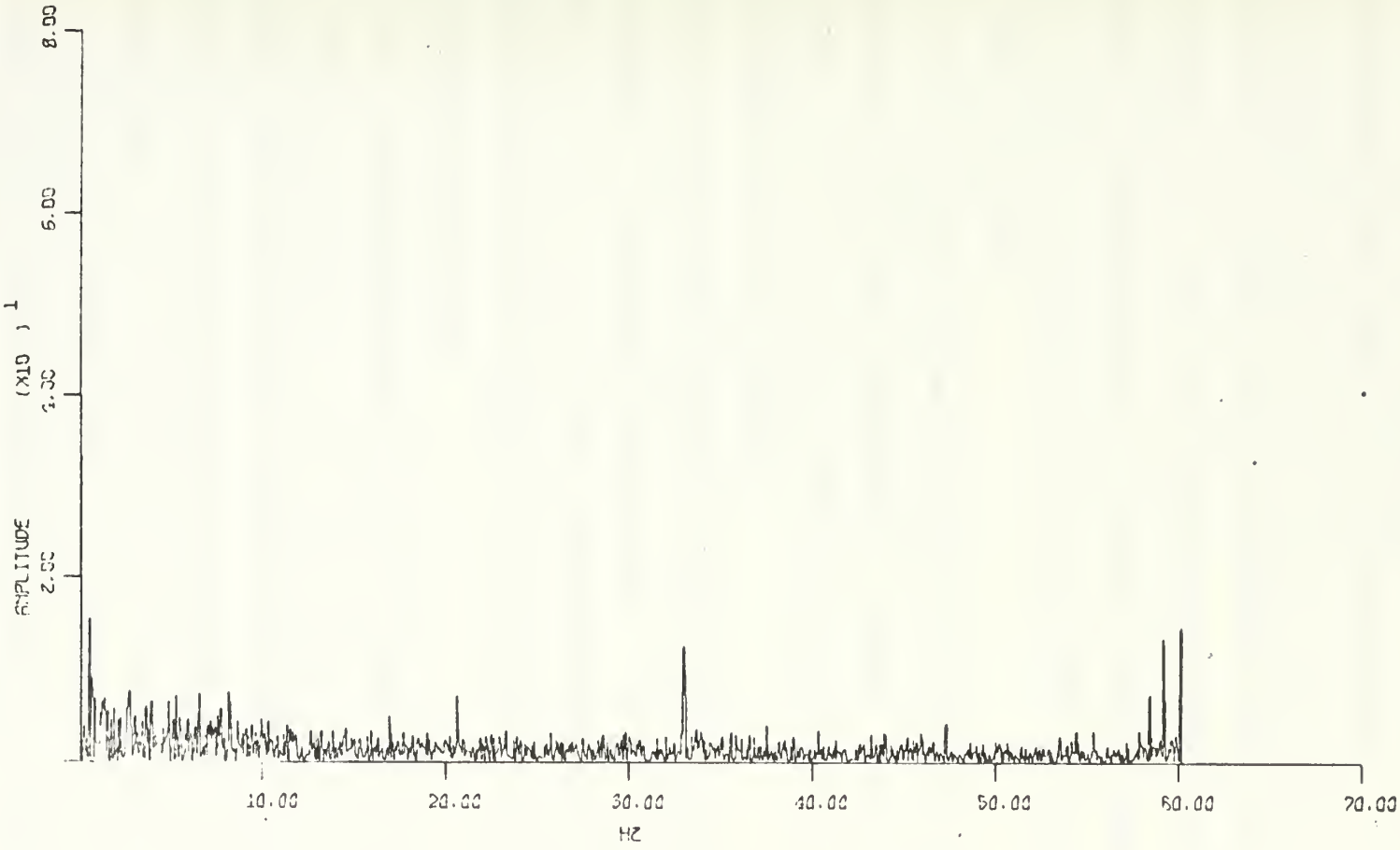


FIGURE 16. Typical Frequency Spectrum of Beam Wander

In addition, a strong component of the beam wander spectrum at about 20 Hz can be seen in Figure 16. This frequency corresponds to the length of the record and sample rate used in the digitizing process. It is believed to be entirely the result of data reduction, since it appeared in practically every file processed, always corresponding to the sampling rate and record length in use. This could probably be eliminated in the WANDER/SPREAD program by recomputing the bias of C2 at every image. However, this would likely increase the magnitude of the 60 cycle jitter and would be extremely costly in CPU time.

Figure 17 shows a plot of beam wander taken using alternate images. As can be seen the 60 cycle jitter is substantially reduced. This indicates that the jitter is at least partly the result of non-uniformity in the scan between the forward and reverse directions.

In general it has been found that better results have been achieved in the data processing if the scan amplitude was small. This allowed more sample points within each image for a given digitizing rate, and thus a better statistical base for data reduction. This is particularly true in the case of computing image shapes.

Table I shows the RMS beam wander values for the data that was processed. The image shapes were not gaussian in most cases, and so are not included. Where the shapes roughly approximated a gaussian distribution, enlarged versions of Figure 14 were used to obtain the half width of the image at its half maximum point. These varied from 2.0 to 11.2 microradians with an average of 4.0 microradians for the eight files for which this was possible. The image shapes with beam wander included varied from 1.5 to greater than 55.0 microradians for six files which were roughly gaussian.

The fact that many of the image shapes appeared skewed is believed primarily due to the receiver not having been located in the center of the

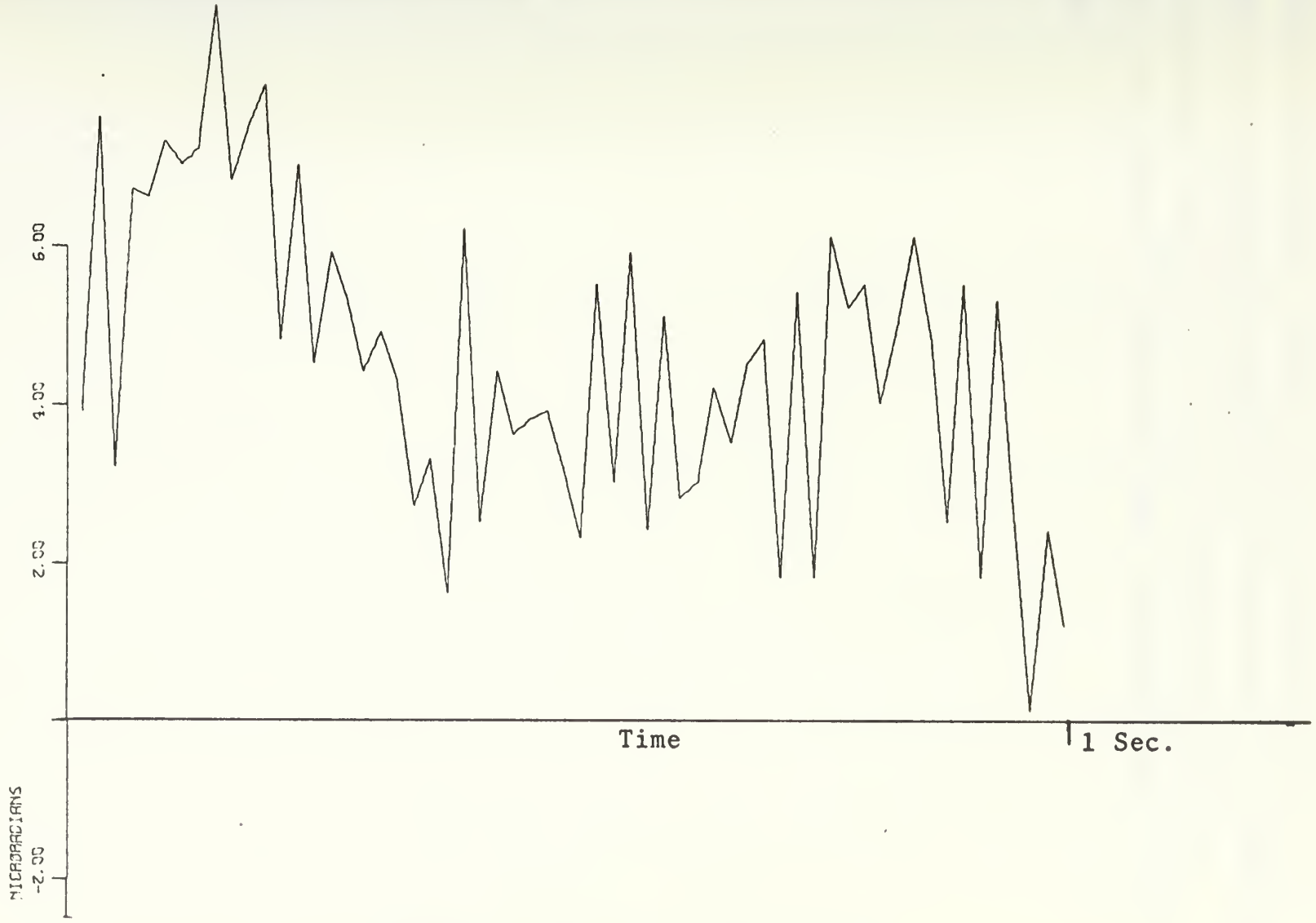


FIGURE 17. One Second of Beam Wander
Using Alternate Images

gaussian distribution. Hallway trials demonstrated the necessity for the telescope being centered. However, this was not always feasible in the field due to the propagation distance and the fact that all the experiments were conducted in conjunction with the scintillation work reported in Ref. 13, the apparatus for which also needed to be near the center of the beam.

TABLE I

| Date | Time | $C_n$ [Ref. 13] | RMS beam Wander | Image half width B.W. Removed | Image half width Not Removed |
|---|---|---|---|---|---|
| 9 Oct | 2049 | - | 4.6 | 2.0 | 2.0 |
| | 2153 | 0.307 | 6.1 | 2.9 | 1.5 |
| | 2216 | 0.294 | 7.8 | - | - |
| | 2255 | 0.271 | 7.8 | 7.7 | - |
| 18 Oct | 2020 | 0.292 | 18.5 | - | - |
| | 2022 | 0.292 | 20.0 | - | - |
| | 2044 | 0.375 | 14.5 | 4.4 | - |
| | 2049 | 0.407 | 13.5 | 4.3 | - |
| | 2122 | 0.503 | 19.5 | 5.3 | 18.2 |
| | 2151 | - | 24.4 | 2.2 | 13.8 |
| 22 Oct | 1626 | 0.506 | 13.0 | 11.2 | 12.8 |
| | 1636 | 0.533 | 12.2 | - | - |
| | 1649 | 0.555 | 30.2 | - | - |
| | 1710 | 0.510 | 13.9 | - | >55 |
| | 1718 | 0.533 | 11.1 | - | - |
| | 1729 | 0.563 | 27.4 | - | - |

All beam wander and half width values in microdians.

All $C_n$ values in $10^{-7}$ $m^{-1/3}$ .

## V. CONCLUSIONS

The system described above successfully operated to its design criteria during the three trials. Consistent measurements of beam wander values in the range of 4.6 to 30.2 microradians and image half widths from 2.0 to 11.2 microradians testify strongly for the resolution of the apparatus.

Thus, there seems no reason why continued development of the system should not go forward with the basic concept, i.e., measurement with a scanning telescope, as a basis.

The experiences related above indicate that the following areas for such development would be the most productive at present.

The telescope should be reconfigured for simultaneous measurement in the visible and infra-red regions.

An automatic tracking system for the telescope needs to be constructed, in order that it may be operated with the shipboard laser stabilization system, which is now nearing completion. This is necessary in order to obtain measurements which are as free as possible of influences due to anomalies in the turbulence conditions brought about by shoreline terrain. In this regard, it should be mentioned that conversations with sailing enthusiasts have indicated that conditions over the Monterey Bay propagation path are not normally homogeneous, but rather that in about the western two-thirds of the path a strong northwesterly breeze usually blows, while in the eastern third of the path, the air is nearly dead calm. In addition, to provide good correlation of data with $C_n$ measurements, a propagation path as nearly perpendicular to the prevailing wind as possible is desirable. The shipboard transmitter will provide the ability to seek out such conditions.

Further improvements in the data processing system would greatly increase the volume of information that could practicably be obtained from experiments. It has been found that with the system described above only about a minute of experimental data can be processed per day, primarily because of competition with other users of the IBM 360. An automated system using a small computer such as those employed in the experiments described in Refs. 14 and 8 would be an excellent solution to this problem.

Finally, it should be noted that the present status of the project is approximately six months ahead of what was planned at the outset. Thus, it would appear that, with continued effort, there is no reason why the remaining work just described cannot be successfully accomplished.

```
//  EXEC  FORTCLG,REGION.GO=100K
//FORT.SYSIN  DD  *
C
C                                        7T09
C
C
C
      DIMENSION IDAT(1024),DAT(1024)
      REWIND 2
      REWIND 4
      NRECL=1024
      FACTOR=1.0/10000.0
      M=0
   11 J=0
   10 READ(2,15,END=50,ERR=60) IDAT
   15 FORMAT(8(128A4))
      J=J+1
      CALL FORM(IDAT,NRECL)
      DO 22 I=1,NRECL
   22 DAT(I)=IDAT(I)*FACTOR
      IF (J.GT.2) GO TO 80
      WRITE (6,70) J
   70 FORMAT('0',10X,'RECORD NO.=',I4)
      WRITE (6,40) DAT
   40 FORMAT (1X,8F12.5)
   80 WRITE (4,15) DAT
      GO TO 10
   60 WRITE (6,61) J
   61 FORMAT('0',5X,'READ ERROR,RECORD NO.=',I4)
      GO TO 10
   50 WRITE (6,51) M,J
   51 FORMAT('0',5X,'END OF FILE',I2,'  NO. RECORDS=',I3)
      END FILE 4
      M=M+1
      IF(M.LT.6) GO TO 11
      WRITE (6,71) M
   71 FORMAT('0',5X,'END OF TAPE, FILES =',I3)
      STOP
      END
//GO.FT02F001  DD  UNIT=2400-1,VOL=SER=BEALL,LABEL=(1,NL,,IN),
//     DISP=(OLD,PASS),DCB=(DEN=1,RECFM=F,BLKSIZE=4096)
//GO.FT02F002  DD  UNIT=AFF=FT02F001,VOL=REF=*.GO.FT02F001,
//     DISP=(OLD,PASS),DCB=(DEN=1,RECFM=F,BLKSIZE=4096),
//     LABEL=(2,NL,,IN)
//GO.FT02F003  DD  UNIT=AFF=FT02F001,VOL=REF=*.GO.FT02F001,
//     DISP=(OLD,PASS),DCB=(DEN=1,RECFM=F,BLKSIZE=4096),
//     LABEL=(3,NL,,IN)
//GO.FT02F004  DD  UNIT=AFF=FT02F001,VOL=REF=*.GO.FT02F001,
```

```
//     DISP=(OLD,PASS),DCB=(DEN=1,RECFM=F,BLKSIZE=4096),
//     LABEL=(4,NL,,IN)
//GO.FTC2F005  DD  UNIT=AFF=FT02F001,VOL=REF=*.GC.FT02F001,
//     DISP=(OLD,PASS),DCB=(DEN=1,RECFM=F,BLKSIZE=4096),
//     LABEL=(5,NL,,IN)
//GO.FT02F006  DD  UNIT=AFF=FT02F001,VOL=REF=*.GO.FT02F001,
//     DISP=(OLD,PASS),DCB=(DEN=1,RECFM=F,BLKSIZE=4096),
//     LABEL=(6,NL,,IN)
//GO.FT04F001  DD  UNIT=2400,VOL=SER=NPS180,DSNAME=BEA91,
//     DISP=(NEW,PASS),DCB=(DEN=2,RECFM=FB,LRECL=4096,BLKSIZE=8192),
//     LABEL=(1,SL,,OUT)
//     DISP=(NEW,PASS),DCB=(DEN=2,RECFM=FB,LRECL=4096,BLKSIZE=8192),
//     LABEL=(2,SL,,OUT),DSNAME=BEA92
//     DISP=(NEW,PASS),DCB=(DEN=2,RECFM=FB,LRECL=4096,BLKSIZE=8192),
//     LABEL=(3,SL,,OUT),DSNAME=BEA93
//     DISP=(NEW,PASS),DCB=(DEN=2,RECFM=FB,LRECL=4096,BLKSIZE=8192),
//     LABEL=(4,SL,,OUT),DSNAME=BEA94
//     DISP=(NEW,PASS),DCB=(DEN=2,RECFM=FB,LRECL=4096,BLKSIZE=8192),
//     LABEL=(5,SL,,OUT),DSNAME=BEA95
//     DISP=(NEW,PASS),DCB=(DEN=2,RECFM=FB,LRECL=4096,BLKSIZE=8192),
//     LABEL=(6,SL,,OUT),DSNAME=BEA96
```

```
//   EXEC  FORTCLGP,REGION.GO=150K
//FORT.SYSIN  DD  *
C
C                        BEAM WANDER/SPREAD
C
C
      DIMENSION DAT(1024),SPREAD(200),WANDER(7000),OFLO1(500),
     /OFLO2(650),C1(512),C2(512),UNFXD(200)
      DATA SPREAD/200*0.0/,WANDER/7000*0.0/,UNFXD/200*0.0/
      REWIND 4
      IERNUM=0
      LSTOP=0
      ICFLO=0
      L=0
      M=1
      READ (5,200) IAP2PI,NCHAN,NSAMP,MAXERR,INTREQ,IBIREQ,IAGREQ,KO
  200 FORMAT(1X,I5,I2,I4,I4,I3,I3,I3,I3)
      WRITE (6,200) IAP2PI,NCHAN,NSAMP,MAXERR, INTREQ,IBIREQ,IAGREQ,KO
      WRITE(6,215) M
  215 FORMAT('0',I4,'   L     M      BIASX        A          IPI IOFLO    BIAS
     /Y              WANDER(M)')
  100 IF (IERNUM.GE.MAXERR) GO TO 730
      IF(L.EQ.0) GO TO 150
      MMIN1=M-1
      WRITE(6,230) L,M,BIASX,A,IPI,IOFLO,BIASY,WANDER(MMIN1)
  230 FORMAT(5X,I4,I5,F10.3,F10.3,4X,I4,I5,F10.3,10X,F10.3)
  150 L=L+1
  300 IF(LSTOP.EQ.1) GO TO 3000
      READ (4,310,END=320,ERR=330) DAT
  310 FORMAT(8(128A4))
      IF(L.GT.2) GO TO 350
      WRITE (6,315) L,(DAT(I),I=1,9)
  315 FORMAT(1X,'REC. NO. ',I4,'FIRST 9 DAT(I)'/1X,9F12.5)
      GO TO 350
  320 LSTOP=1
      WRITE(6,321) L
  321 FORMAT(1X,'LAST RECORD OF FILE. RECORD NO. ',I4)
      GO TO 350
  330 WRITE (6,331) L
  331 FORMAT(1X,'READ ERROR ON RECORD NO. ',I4)
      GO TO 100
  350 DO 351 I=1,NSAMP
      IFAC=NCHAN*(I-1)
      C1(I)=DAT(IFAC+1)
      C2(I)=DAT(IFAC+2)
  351 CONTINUE
  360 IF(L.GT.3) GO TO 380
      WRITE (6,365)L,C1(1),C1(NSAMP),C2(1),C2(NSAMP)
  365 FORMAT(1X,'FIRST AND LASTSAMPLES, REC. NO. ',I4,'FOR C1 ',2F12.5,'
```

```
   / FOR C2 ',2F12.5)
380 DO 400 I=2,IAP2PI
    IF (C2(I).GE.C2(I-1).AND.C2(I).GE.C2(I+1)) GO TO 420
400 CONTINUE
    GO TO 700
420 IF(I.EQ.2) GO TO 430
    JSUM=15
    IF(I.LE.15) JSUM=I-1
    DO 421 J=1,JSUM
    IF(C2(I).LT.C2(I-J)) GO TO 400
421 CONTINUE
430 DO 431 J=1,15
    IF(C2(I).LT.C2(I+J)) GO TO 400
431 CONTINUE
    IC2MAX =I
    C2MAX=C2(I)
    DO 500 I=2,IAP2PI
    IF(C2(I).LE.C2(I-1).AND.C2(I).LE.C2(I+1)) GO TO 520
500 CONTINUE
    GO TO 710
520 IF(I.EQ.2) GO TO 530
    JSUM=15
    IF(I.LE.15) JSUM=I-1
    DO 521 J=1,JSUM
    IF(C2(I).GT.C2(I-J)) GO TO 500
521 CONTINUE
530 DO 531 J=1,15
    IF(C2(I).GT.C2(I+J)) GO TO 500
531 CONTINUE
    IC2MIN=I
    C2MIN=C2(I)
    IPI=IABS(IC2MAX-IC2MIN)
    IF(L.EQ.1) GO TO 650
    APCTBD=(((C2MAX-C2MIN)/2.0-A)/A)*100.0
    IF(ABS(APCTBD).LE.10.0) GO TO 650
    WRITE (6,605) L,APCTBD
605 FORMAT(1X,'RECORD NO. ',I4,' A VARIES MORE THAN 10 PCT.
   / PCT. VARIATION= ',F10.2)
    GO TO 100
650 A=(C2MAX-C2MIN)/2.0
    BIASX=C2MAX-A
    DO 655 I=1,NSAMP
    C2(I)=C2(I)-BIASX
655 CONTINUE
    ISHMIN=2
    ISHMAX=IPI+IAGREQ
660 DO 665 I=ISHMIN,ISHMAX
    IF(ABS(C2(I-1)).GT.ABS(C2(I)).AND.ABS(C2(I+1)).GT.ABS(C2(I))) GO T
```

```
     /O 666
  665 CCNTINUE
      GO TO 670
  666 IF(ABS(C2(I-2)).GT.ABS(C2(I-1)).AND.ABS(C2(I+2)).GT.ABS(C2(I+1)))
     /GC TO 1000
      GO TO 665
  670 IERNUM=IERNUM+1
      IF(IERNUM.GE.MAXERR) GC TO 730
      WRITE(6,675) M
  675 FCRMAT(1X,'UNABLE TO FIND ZERO OF X FOR IMAGE NO. ',I5,' SKIPPING
     / THAT ONE')
      WRITE(6,676) IOFLO,ISHMIN,BIASX,A
  676 FCRMAT(1X,'IOFLO=',I4,'ISHMIN=',I4,' BIASX=',F10.5,' A=',F10.5,'C2
     / FROM ISHMIN TO ISHMAX IS:')
      WRITE(6,677)(C2(I),I=ISHMIN,ISHMAX)
  677 FCRMAT(1X,10F10.5)
      WRITE(6,678) M
  678 FCRMAT('0',I4,'  L     M      BIASX        A          IPI IOFLO    BIAS
     /Y              WANDER(M)')
      M=M+1
  68C ISHMIN=ISHMIN+IPI
      ISHMAX=ISHMAX+IPI
      ICFLO=0
      IF(ISHMIN.LT.2) GO TO 690
      IF(ISHMAX.GT.NSAMP-2) GO TO 690
      GC TO 660
  69C WRITE(6,691) L
  691 FCRMAT('0','SEARCH LIMIT EXCEEDED. SKIPPING RECORD NC.',I5)
      IERNUM=IERNUM+1
      GC TO 100
  700 WRITE (6,705) L
  705 FCRMAT(1X,'UNABLE TO FIND MAX OF CHANNEL 2 FOR RECORD NO. ',I4,'
     /WENT TO NEXT RECORD')
      ICFLO=0
      GC TO 740
  71C WRITE (6,715) L
  715 FCRMAT(1X,'UNABLE TO FIND MIN OF CHANNEL 2 FOR RECORD NO. ',I4,'
     /WENT TO NEXT RECORD')
      IOFLO=0
      GC TO 740
  72C WRITE(6,725) L
  725 FCRMAT (1X,'UNABLE TO FIND PERIOD OF CHANNEL 2 FOR RECORD NO.',I4,
     /'WENT TO NEXT RECORD')
      GC TO 740
  730 WRITE (6,735) IERNUM
  735 FCRMAT (1X,'WE ARE IN TROUBLE BOSS. FAILURES ON CH. 2= ',I4)
      GO TO 3000
  740 IERNUM=IERNUM+1
```

```
      GO TO 100
1000  IO=I
      IF(L.EQ.1.AND.IO.LE.INTREQ) GO TC 680
1010  IF(IOFLO.NE.0) GO TO 1500
1020  IF (IO+INTREQ.GT.NSAMP) GO TO 2000
      INTMIN=IC-INTREQ
      INTMAX=IO+INTREQ
      BISUM=0.0
      IF(INTMIN-1.LT.IBIREQ) GO TO 1050
      IBIMIN=INTMIN-IBIREQ
      DC 1025 I=IBIMIN,INTMIN
      BISUM=BISUM+C1(I)
1025  CONTINUE
      BIASY=BISUM/FLOAT(IBIREQ+1)
      GO TO 1100
1050  IBIMAX =INTMAX +IBIREQ
      DC 1055 I=INTMAX,IBIMAX
      BISUM=BISUM+C1(I)
1055  CCNTINUE
      BIASY=BISUM/FLOAT(IBIREQ+1)
1100  DO 1105 I=INTMIN,INTMAX
      C1(I)=C1(I)-BIASY
1105  CONTINUE
      IF (IO+IPI+IAGREQ.GE.NSAMP) GO TO 1200
      ISHMIN=IO+IPI-IAGREQ
      ISHMAX=IO+IPI+IAGREQ
      IF (ISHMIN.LT.2) GO TO 1160
      DC 1155 I=ISHMIN,ISHMAX
      IF(ABS(C2(I-1)).GT.ABS(C2(I)).AND.ABS(C2(I+1)).GT.ABS(C2(I))) GO T
     /C 1170
1155  CCNTINUE
      GO TO 670
1160  WRITE(6,1161) L
1161  FORMAT('0','SEARCH LIMIT EXCEEDED. SKIPPING RECORD NO.',I5)
      IERNUM=IERNUM+1
      GC TO 100
1170  IF(ABS(C2(I-2)).GT.ABS(C2(I-1)).AND.ABS(C2(I+2)).GT.ABS(C2(I+1)))
     /GC TO 1180
      GC TO 1155
1180  IPI=I-IO
1200  IF(INTMAX+IPI/2.GT.NSAMP) GO TO 1220
      IDX=IPI/2
      GO TO 1230
1220  IDX=-2*IPI+IPI/2
1230  FSTMOM=0.0
      AREAIM=0.0
      DC 1235 I=INTMIN,INTMAX
      FSTMOM=FSTMOM+C1(I)*C2(I)*C2(I+IDX)
```

```
      AREAIM=AREAIM+C1(I)*C2(I+IDX)
 1235 CONTINUE
      YMEAN=FSTMOM/AREAIM
      WANDER(M)=YMEAN
 1260 DO 1265 I=INTMIN,INTMAX
      K=IFIX(C2(I)-YMEAN)+KO
      IF(K.LT.1.OR.K.GT.2*KC) GO TO 1265
      SPREAD(K)=SPREAD(K)+C1(I)
      N=IFIX(C2(I))+KO
      IF(N.LT.1.OR.N.GT.2*KC) GO TO 1265
      UNFXD(N)=UNFXD(N)+C1(I)
 1265 CONTINUE
 1270 CONTINUE
      M=M+1
      IO=IO+IPI
      GO TO 1020
 1500 IOF1MX=2*INTREQ+IBIREQ+2-IOFLO
      DO 1515 I=1,IOF1MX
      OFLO1(IOFLO+I)=C1(I)
 1515 CONTINUE
      IOF2MX=INTREQ+IPI+2*IAGREQ+IBIREQ-IOFLO
      DO 1525 I=1,IOF2MX
      OFLO2(IOFLO+I)=C2(I)
 1525 CONTINUE
      IF(IO.LE.IOF1MX) JO=IOFLO+IO
      INTMIN =JO-INTREQ
      INTMAX=JO+INTREQ
      BISUM=0.0
      DO 1535 J=1,INTMIN
      BISUM=BISUM+OFLO1(J)
 1535 CONTINUE
      BIASY=BISUM/FLOAT(INTMIN)
      DO 1545 J=INTMIN,INTMAX
      OFLO1(J)=OFLO1(J)-BIASY
 1545 CONTINUE
      IF(IO.LE.IOF1MX) GO TO 1560
      IPI=IOFLO+IO-JO
      GO TO 1600
 1560 ISHMIN=JO+IPI-IAGREQ
      ISHMAX=JO+IPI+IAGREQ
      IF(ISHMIN.LT.2.OR.ISHMAX.GT.IOF2MX+IOFLO-2) GO TO 1576
      DO 1575 J=ISHMIN,ISHMAX
      IF(ABS(OFLO2(J-1)).GT.ABS(OFLO2(J)).AND.ABS(OFLO2(J+1)).GT.ABS(OFL
     /O2(J))) GO TO 1580
 1575 CONTINUE
      ISHMIN=ISHMIN-IOFLO
      ISHMAX=ISHMAX-IOFLO
      GO TO 670
```

```
1576 WRITE(6,1577) L
1577 FORMAT('0','SEARCH LIMIT EXCEEDED. SKIPPING RECORD NO.',I5)
     IERNUM=IERNUM+1
     ICFLO=0
     GO TO 100
1580 IF(ABS(OFLO2(J-2)).GT.ABS(OFLO2(J-1)).AND.ABS(OFLO2(J+2)).GT.ABS(O
    /FLO2(J+1))) GO TO 1590
     GO TO 1575
1590 IPI=J-JO
     IO=IO+IPI
1600 IDX=IPI/2
     FSTMOM=0.0
     AREAIM=0.0
     DO 1625 I=INTMIN,INTMAX
     FSTMOM=FSTMOM+OFLO1(I)*OFLO2(I+IDX)*OFLO2(I)
     AREAIM=AREAIM+OFLO1(I)*OFLO2(I+IDX)
1625 CONTINUE
     YMEAN=FSTMOM/AREAIM
     WANDER(M)=YMEAN
1660 DO 1665 J=INTMIN,INTMAX
     K=IFIX(OFLO2(J)-YMEAN)+KO
     IF(K.LT.1.OR.K.GT.2*KO) GO TO 1665
     SPREAD(K)=SPREAD(K)+OFLO1(J)
     N=IFIX(OFLO2(J))+KO
     IF(N.LT.1.OR.N.GT.2*KO) GO TO 1665
     UNFXD(N)=UNFXD(N)+OFLO1(J)
1665 CONTINUE
1670 M=M+1
     ICFLO=0
     GO TO 1020
2000 IF(IO-INTREQ.GT.NSAMP) GO TO 100
     ICVFST=IO-INTREQ-IBIREQ
     DO 2015 I=ICVFST,NSAMP
     J=I-ICVFST+1
     OFLO1(J)=C1(I)
     OFLO2(J)=C2(I)
2015 CONTINUE
     ICFLO=NSAMP-ICVFST+1
     JC=IC-ICVFST+1
     GO TO 100
3000 ESTPD=2.0*(FLOAT((L-1)*NSAMP/M))
     WRITE(6,3015) M,ESTPD
3015 FORMAT(1X,'NO. OF IMAGES PROCESSED= ',I5,'ESTIMATE PERIOD OF SINE
    /WAVE= ',F10.2)
     WRITE(6,3025) M,KO
3025 FORMAT('0','AVERAGE SHAPE FOR',I5,' IMAGES WITH CENTROIDS AT ',I3,
    /'TH DATA POINT SHOWN')
     WRITE(6,3026) SPREAD
```

```
3026 FORMAT(1X,7E16.7)
     WRITE(6,3045) M
3045 FORMAT('0','AVERAGE IMAGE SHAPE FOR ',I5,'IMAGESWITHOUT WANDER
    /REMOVED IS')
     WRITE(6,3046) UNFXD
3046 FORMAT(7E16.7)
     WRITE(6,3035) M
3035 FORMAT('0','BEAM WANDER FOR',I5,'IMAGES IS')
     WRITE(6,3036)(WANDER(I),I=1,M)
3036 FORMAT(10F7.1)
     WRITE(7,3055)(WANDER(I),I=1,M)
3055 FORMAT(10F7.1)
     WRITE(7,3056) SPREAD
3056 FORMAT(4E16.7)
     WRITE(7,3057) UNFXD
3057 FORMAT(4E16.7)
     WANSUM=0.0
     DO 3060 I=1,M
     WANSUM=WANSUM+WANDER(I)
3060 CONTINUE
     WMEAN=WANSUM/FLOAT(M)
     VARSUM=0.0
     DO 3070 I=1,M
     VARSUM=VARSUM+(WANDER(I)-WMEAN)**2
3070 CONTINUE
     WANRMS=SQRT(VARSUM/FLOAT(M))
     WRITE(6,3080) M,WANRMS,WMEAN
3080 FORMAT('0','RMS BEAM WANDER FOR ',I5,' IMAGES IS ',F10.3,' MEAN IS
    / ',F10.3)
     REWIND 4
     STOP
     END
//GO.FT06F001  DD  SPACE=(CYL,(1,1)),SYSOUT=O
//GO.FT04F001  DD  UNIT=2400,VOL=SER=NPS180,
//     DCB=(DEN=2,RECFM=FB,LRECL=4096,BLKSIZE=8192),
//     DSNAME=BEA91,LABEL=(1,SL,,IN)
//GO.SYSIN  DD  *
```

```
//   EXEC  FORTCLGP,REGION.GO=100K
//FORT.SYSIN  DD  DSNAME=SSP3(RHARM),DISP=SHR
//   DD  *
C
C                                    BEAT
C
C
C
C N=2**M. DIM(A)=2*N+4. DIM(INV)=DIM(S)=(1/8)*2*N. TAKES 2*N DATA PTS.
C FRQINC IS THE NUMBER OF FREQUENCIES IT IS DESIRED TO HAVE
C IN ONE INCH OF THE PLOT.
C FRQCAL IS SUCH THAT THE DESIRED LENGTH OF THE PLOT=FRQCAL
C TIMES THE NUMBER OF SAMPLE POINTS DIVIDED BY FRQINC.
      DIMENSION A(1028),INV(128),S(128),FREQ(1028)
      DATA A/1028*0.0/,INV/128*0/,S/128*0.0/
      IFERR=0
      READ(5,50) FRQCAL,FRQINC,M
   50 FORMAT(2F10.4,I2)
      WRITE(6,50) FRQCAL,FRQINC,M
C ECHO CHECK
      READ(5,60) DATFIL
   60 FORMAT(F10.1)
      WRITE (6,60) DATFIL
      READ(5,100) A
  100 FORMAT(10F7.1)
      CALL RHARM(A,M,INV,S,IFERR)
      WRITE (6,300) A
  300 FORMAT('0',5(5X,2F10.3))
      A(1027)=0.0
      A(1028)=0.0
      NPTS=2*(2**M)+4
      DO 500 I=1,NPTS
      FREQ(I)=FRQCAL*FLOAT(I)
      A(I)=ABS(A(I))
  500 CONTINUE
      XMAX=FRQCAL*FLOAT(NPTS)/FRQINC
      CALL SCALE(FREQ,NPTS,1,XMAX,0.0,FMIN,DF)
      CALL SCALE(A,NPTS,1,3.0,0.0,AMIN,DA)
      FMIN=0.0
      DF=FRQINC
      CALL PLOTS
      CALL AXIS(0.0,0.0,'HZ',-2,7.0,0.0,FMIN,DF)
      CALL AXIS(0.0,0.0,'AMPLITUDE',9,3.5,90.0,AMIN,DA)
      CALL LINE(FREQ,A,NPTS,1,1)
      CALL SYMBOL(0.0,5.0,0.21,'BEAT1570',0.0,8)
      CALL NUMBER(4.0,5.0,0.21,DATFIL,0.0,-1)
      CALL PLOT(0.0,12.0,-3)
      CALL PLOTE
```

```
      STOP
      END
//GC.SYSIN  DD  *
```

```
//  EXEC  FORTCLGP,REGION.GO=100K
//FORT.SYSIN  DD  *
C                                        BEAD
C
C
C  BEAD PLOTS TIME AVERAGE IMAGE SHAPE WITH AND WITHOUT BEAM
C  WANDER AND THREE INTERVALS OF BEAM WANDER.
C
C  WCAL AND SCAL ARE REAL*4'S SUCH THAT A*WCAL=A*SCAL=AMPLITUDE OF
C  SCAN DRIVE SIGNAL IN MICRORADIANS, WHERE A= RAW AMPLITUDE OF C2
C  FROM PROGRAM WANDER/SPREAD.
C  TCAL IS A REAL*4 SUCH THAT TCAL*NWPTS=INTERVAL OF TIME WHICH
C  IS DESIRED FOR BEAM WANDER PLOT.
C  NSPTS=DIM(SPREAD) FROM WANDER/SPREAD.
C  NWPTS = DESIRED NUMBER OF BEAM WANDER VALUES TO BE PLOTTED.
C
C
C  DIM(WANDER)=3*NWPTS.
C  DIM(W)=NWPTS.
C  DIM(X)=DIM(SPREAD)=DIM(UNFXD)=DIMENSION OF LATTER TWO IN
C  PROGRAM WANDER/SPREAD.
C
C
      DIMENSION WANDER(360),W(120),SPREAD(200),UNFXD(200),X(200),
     /T(120)
      READ(5,100) WCAL,SCAL,TCAL,NSPTS,NWPTS
  100 FORMAT(2F10.3,F10.6,2I10)
      WRITE(6,100) WCAL,SCAL,TCAL,NSPTS,NWPTS
      READ(5,120) WANDER
  120 FORMAT(10F7.1)
      READ(5,140) SPREAD
  140 FORMAT(4E16.7)
      READ(5,160) UNFXD
  160 FORMAT(4E16.7)
      DO 180 I=1,NSPTS
      X(I)=(FLOAT(I))*SCAL
  180 CONTINUE
      CALL SCALE(X,NSPTS,1,7.0,0.0,XMIN,DX)
      CALL SCALE(SPREAD,NSPTS,1,5.0,0.0,SMIN,DS)
      CALL PLOTS
      CALL AXIS(0.0,0.0,'MICRORADIANS',-12,7.5,0.0,XMIN,DX)
      CALL AXIS(0.0,0.0,'INTENSITY',9,5.5,90.0,SMIN,DS)
      CALL LINE(X,SPREAD,NSPTS,1,-7)
      CALL SYMBOL(0.0,6.5,0.21,'BEALL',0.0,5)
      CALL SYMBOL(0.0,6.0,0.21,'IMAGE SHAPE WITHOUT WANDER',0.0,26)
      CALL PLOT(0.0,12.0,-3)
      CALL PLOTE
      CALL SCALE(UNFXD,NSPTS,1,5.0,0.0,SMIN,DS)
```

```
      CALL PLOTS
      CALL AXIS(0.0,0.0,'MICRORADIANS',-12,7.5,0.0,XMIN,DX)
      CALL AXIS(0.0,0.0,'INTENSITY',9,5.5,90.0,SMIN,DS)
      CALL LINE(X,UNFXD,NSPTS,1,-7)
      CALL SYMBOL(0.0,6.5,0.21,'BEALL',0.0,5)
      CALL SYMBOL(0.0,6.0,0.21,'THETA PRIME',0.0,11)
      CALL PLOT(0.0,12.0,-3)
      CALL PLOTE
      DO 200 I=1,NWPTS
      T(I)=(FLOAT(I))*TCAL
  200 CONTINUE
      CALL SCALE(T,NWPTS,1,7.0,0.0,TMIN,DT)
      DO 1000 J=1,3
      JFACT=(J-1)*NWPTS
      DO 220 I=1,NWPTS
      W(I)=WANDER(JFACT+I)
      W(I)=WCAL*W(I)
  220 CONTINUE
      CALL SCALE(W,NWPTS,1,5.0,0.0,WMIN,DW)
      CALL PLOTS
      CALL AXIS(0.0,-2.5,'TIME',-4,8.0,0.0,TMIN,DT)
      CALL AXIS(0.0,-2.5,'MICRORADIANS',12,6.0,90.0,WMIN,DW)
      CALL LINE(T,W,NWPTS,1,1)
      CALL SYMBOL(0.0,7.5,0.21,'BEAM WANDER FOR SECOND NO.',0.0,26)
      FJ=FLOAT(J)
      CALL NUMBER(5.0,7.5,0.21,FJ,0.0,-1)
      CALL SYMBOL(0.0,8.0,0.21,'BEALL',0.0,5)
      CALL PLOT(0.0,12.0,-3)
      CALL PLOTE
 1000 CONTINUE
      STOP
      END
//GO.SYSIN  DD  *
```

## BIBLIOGRAPHY


1. Strohbehn, J. W., "Line-of-Sight Wave Propagation Through the Turbulent Atmosphere," Proceedings of the IEEE, v. 56, p. 1301-1318, August 1968.

2. Tatarski, V. I., Wave Propagation in a Turbulent Medium, McGraw-Hill, 1961.

3. Haagensen, B. G., Laser Beam Scintillation in the Marine Boundary Layer, M.S. Thesis, U. S. Naval Postgraduate School, Monterey, 1972

4. Dowling, J. A. and Livingston, P. M., "Behavior of Focused Beams in Atmospheric Turbulence: Measurements and Comments on the Theory," Journal of the Optical Society of America, v. 63, p. 846-858, July 1973.

5. Varvatsis, A. D. and Sancer, M. I., "Expansion of a Focused Laser Beam," Canadian Journal of Physics, v. 49, p. 1233, May 1971.

6. Brown, W. P., "Second Moment of a Wave Propagating in a Random Medium," Journal of the Optical Society of America, v. 61, p. 1051, August 1971.

7. Yura, H. T., "First and Second Moments of an Optical Wave Propagating in a Random Medium: Equivalence of the Solution of the Dyson and Blythe Salpeter Solution to that observed by a Huygens-Fresnel Principle," Journal of the Optical Society of America, v. 62, p. 889, 1972.

8. Chiba, T., "Spot Dancing of the Laser Beam Propagated Through the Turbulent Atmosphere," Applied Optics, v. 10, p. 2456, 1971.

9. Alcaraz, E. C. and Livingston, P. M., Proceedings Electro-Optical Design Conference, 1972, Industrial and Scientific Management, Inc., Chicago, p. 76, 1972.

10. Fried, D. C., "Resolution Through Random Inhomogeneous Medium," Journal of the Optical Society of America, v. 56, p. 1372, October 1966.

11. Hildebrand, W. T., An Optical Apparatus To Determine The Effect of Turbulence on the Modulation Transfer Function of the Atmosphere, M.S. U. S. Naval Postgraduate School, Monterey, 1972.

12. Resnick, R. and Halliday, D., Physics, Wiley, p. 372, 1966.

13. Schroeder, A. F., Laser Scintillation Properties in the Marine Boundary Layer, M.S. Thesis, U.S. Naval Postgraduate School, Monterey, 1973.

14. Scientific Data Systems, SDS 9300 Computer Reference Manual, 1969.

15. DeLaura, R. D., Electrical Engineering Computer Laboratory Manual for the FORTRAN User, U. S. Naval Postgraduate School Department of Electrical Engineering, 1972.

16. U. S. Naval Postgraduate School Technical Note No. 0211-08, Procedures for Converting 7-Track Magnetic Tapes to 9-Track Magnetic Tapes, Raney, S. D., February 1973.

17. IBM Systems Reference Library Form C28-6539-9, IBM System/360 Operating System Job Control Language, July 1969.

18. Isaacson, E. and Keller, H. B., Analysis of Numerical Methods, Wiley, p. 316, 1966.

19. U. S. Naval Postgraduate School Technical Note No. 0211-03, Plotting Package for NPS IBM 360/67, Johnson, P. C., February 1969.

20. Cooley, J. W. and Tukey, J. W., "An Algorithm for the Machine Calculation of Complex Fourier Series," Mathematics of Computations, v. 19, p. 297, April 1965.

## INITIAL DISTRIBUTION LIST

| | | No. Copies |
|---|---|---|
| 1. | Defense Documentation Center<br>Cameron Station<br>Alexandria, Virginia 22314 | 2 |
| 2. | Library, Code 0212<br>Naval Postgraduate School<br>Monterey, CA 93940 | 2 |
| 3. | Professor O. Heinz, Chairman, Code 61Hz<br>Department of Physics and Chemistry<br>Naval Postgraduate School<br>Monterey, CA 93940 | 1 |
| 4. | Professor E. C. Crittenden, Jr., Code 61Ct<br>Department of Physics and Chemistry<br>Naval Postgraduate School<br>Monterey, CA 93940 | 1 |
| 5. | LCDR David A. Beall, USN<br>USS KILAUEA (AE-26)<br>FPO San Francisco, CA 96601 | 1 |

| REPORT DOCUMENTATION PAGE | | READ INSTRUCTIONS BEFORE COMPLETING FORM |
|---|---|---|
| 1. REPORT NUMBER | 2. GOVT ACCESSION NO. | 3. RECIPIENT'S CATALOG NUMBER |
| 4. TITLE (and Subtitle)<br>An Experiment to Measure Laser Beam Wander and Beam Spread In The Marine Boundary Layer Near Shore | | 5. TYPE OF REPORT & PERIOD COVERED<br>Master's Thesis; December 1973<br>6. PERFORMING ORG. REPORT NUMBER |
| 7. AUTHOR(s)<br>David Albert Beall | | 8. CONTRACT OR GRANT NUMBER(s) |
| 9. PERFORMING ORGANIZATION NAME AND ADDRESS<br>Naval Postgraduate School<br>Monterey, California 93940 | | 10. PROGRAM ELEMENT, PROJECT, TASK AREA & WORK UNIT NUMBERS |
| 11. CONTROLLING OFFICE NAME AND ADDRESS<br>Naval Postgraduate School<br>Monterey, California 93940 | | 12. REPORT DATE<br>December 1973<br>13. NUMBER OF PAGES<br>94 |
| 14. MONITORING AGENCY NAME & ADDRESS(if different from Controlling Office)<br>Naval Postgraduate School<br>Monterey, California 93940 | | 15. SECURITY CLASS. (of this report)<br>Unclassified<br>15a. DECLASSIFICATION/DOWNGRADING SCHEDULE |

16. DISTRIBUTION STATEMENT (of this Report)

Approved for public release; distribution unlimited.

17. DISTRIBUTION STATEMENT (of the abstract entered in Block 20, if different from Report)

18. SUPPLEMENTARY NOTES

19. KEY WORDS (Continue on reverse side if necessary and identify by block number)

20. ABSTRACT (Continue on reverse side if necessary and identify by block number)

A system to measure laser beam wander and beam spread in the atmosphere over the ocean has been designed, constructed, and tested. The apparatus employed a high resolution scanning telescope with a potential for use in a broad range of visual and infra-red wavelengths, and with the ability to measure beam wander and beam spread variations on the order of a few microdians in angle of incidence. Three successful trials with a propagation path over the southern end of Monterey Bay were conducted. Data

was processed using analog and digital computers. RMS values of beam wander from 4.6 to 30.2 microradians were observed.